12

VSC-TR-81-20

REGIONAL DISCRIMINATION RESEARCH

T. J. Bennett
D. G. Lambert
J. R. Murphy
J. M. Savino
C. B. Archambeau

SYSTEMS, SCIENCE AND SOFTWARE
P. O. Box 1620
La Jolla, California 92038

INTERIM FINAL REPORT

June 1981

APPROVED FOR PUBLIC RELEASE,
UNLIMITED DISTRIBUTION

Monitored By:

VELA Seismological Center
312 Montgomery Street
Alexandria, VA 22314

UNCLASSIFIED

SECURITY CLASSIFICATION OF THIS PAGE (When Data Entered)

REPORT DOCUMENTATION PAGE	READ INSTRUCTIONS BEFORE COMPLETING FORM
1. REPORT NUMBER: VSC-TR-81-20	2. GOVT ACCESSION NO.: AD-A112106
	3. RECIPIENT'S CATALOG NUMBER:
4. TITLE (and Subtitle): REGIONAL DISCRIMINATION RESEARCH	5. TYPE OF REPORT & PERIOD COVERED: Interim Final Report 5/1/80 - 3/31/81
	6. PERFORMING ORG. REPORT NUMBER: SSS-R-81-5032
7. AUTHOR(s): T. J. Bennett, D. G. Lambert, J. R. Murphy, J. M. Savino, C. B. Archambeau	8. CONTRACT OR GRANT NUMBER(s): F08606-80-C-0016
9. PERFORMING ORGANIZATION NAME AND ADDRESS: Systems, Science and Software, P. O. Box 1620, La Jolla, California 92038	10. PROGRAM ELEMENT, PROJECT, TASK AREA & WORK UNIT NUMBERS: Program Code No. 6H189, ARPA Order No. 2551
11. CONTROLLING OFFICE NAME AND ADDRESS: VELA Seismological Center, 312 Montgomery Street, Alexandria, Virginia 22314	12. REPORT DATE: June 1981
	13. NUMBER OF PAGES: 77
14. MONITORING AGENCY NAME & ADDRESS (if different from Controlling Office)	15. SECURITY CLASS. (of this report): Unclassified
	15a. DECLASSIFICATION/ DOWNGRADING SCHEDULE

16. DISTRIBUTION STATEMENT (of this Report)

Approved for Public Release, Unlimited Distribution.

17. DISTRIBUTION STATEMENT (of the abstract entered in Block 20, if different from Report)

18. SUPPLEMENTARY NOTES

19. KEY WORDS (Continue on reverse side if necessary and identify by block number)

Regional discrimination
Regional seismic phases
Propagation of regional phases
Eurasian earthquakes and explosions
NTS explosions
Spectral discriminants
Narrow band filtering

20. ABSTRACT (Continue on reverse side if necessary and identify by block number)

The objective of the regional discrimination research project is to systematically assess the potential of regional phases for discriminating earthquakes and nuclear explosions with particular emphasis on defining the applicability of such discriminants to events in various regions of the U.S.S.R. The research program includes two distinct approaches. The first employs more traditional, time domain amplitude and period measurements to compare-

DD FORM 1 JAN 73 1473 A EDITION OF 1 NOV 65 IS OBSOLETE

UNCLASSIFIED

SECURITY CLASSIFICATION OF THIS PAGE (When Data Entered)

ABSTRACT (continued)

the relative excitation of different regional phases from earthquakes and explosions. The second approach focuses on the evaluation of the capabilities of other measurement or processing techniques, such as spectral ratios or narrow-band filtering, to identify seismic sources using regional phases.

The principal technical phases of the regional discrimination research effort are~~as follows~~: (1) review and assess time and frequency domain characteristics of regional seismic phases and evaluate their dependency on source type, propagation path and station environment; (2) Develop a tentative set of source identification criteria based on information from regional phases; (3) Test proposed regional discriminants on observed data to determine their capability to identify earthquakes and explosions in various tectonic and geologic settings.

AFTAC Project Authorization No. VT/0701/B/PMP

ARPA Order No. 2551, Program Code No. 6H189

Effective Date of Contract: 1 April 1981

Contract Expiration Date: 30 September 1982

Amount of Contract: $1,004,347.00

Contract No. F8606-80-C-0016

Principal Investigators and Phone Nos.

Dr. John M. Savino, (714) 453-0060, Ext. 453

Mr. John R. Murphy, (703) 476-5197

Project Scientist and Phone No.

Mr. Brian W. Barker, (202) 325-7581

This research was supported by the Advanced Research Projects Agency of the Department of Defense and was monitored by AFTAC/VSC, Patrick Air Force Base, Florida, 32925, under Contract No. F08606-80-C-0016.

S^3 Project No. 11143

TABLE OF CONTENTS

TABLE OF CONTENTS (continued)

LIST OF ILLUSTRATIONS

LIST OF ILLUSTRATIONS (continued)

LIST OF ILLUSTRATIONS (continued)

LIST OF ILLUSTRATIONS (continued)

I. INTRODUCTION

The objective of the regional discrimination research project is to systematically assess the potential of regional phases for discriminating earthquakes and nuclear explosions with particular emphasis on defining the applicability of such discriminants to events in various regions of the U.S.S.R. The research program includes two distinct approaches. The first employs more traditional, time domain amplitude and period measurements to compare the relative excitation of different regional phases from earthquakes and explosions. The second approach focuses on the evaluation of the capabilities of other measurement or processing techniques, such as spectral ratios or narrow-band filtering, to identify seismic sources using regional phases.

The principal technical phases of the regional discrimination research effort are as follows:

- Review and assess the time and frequency domain characteristics of regional seismic phases and evaluate their dependency on source type, propagation path and station environment.
- Develop a tentative set of source identification criteria based on information from regional phases.
- Test proposed regional discriminants on observed data to determine their capability to identify earthquakes and explosions in various tectonic and geologic settings.

In Section II, the Technical Discussion, we describe our research accomplishments to date on the current project. The impact of our current results on research efforts anticipated under the continuation contract is outlined in Section III. A description of the results of our analysis of seismograms for Eurasian events recorded at AEDS stations is presented in a separate appendix to this report.

II. TECHNICAL DISCUSSION

2.1 REVIEW OF LITERATURE ON REGIONAL PHASE PROPAGATION FROM RUSSIAN EVENTS

2.1.1 Introduction

Much of the interest in the possible use of regional phases in discriminating between underground nuclear explosions and earthquakes stems from observational data which suggests that in certain tectonic environments such phases produce the largest amplitude out to between 20° and 30° from the source. For smaller events, regional phases in this distance range may produce the only detectable signal. In the following, we summarize the state of our understanding of regional phase characteristics in the U.S.S.R. as derived from observational data. The characteristics include propagation and attenuation of regional phases as well as studies involving their application to discrimination.

2.1.2 Propagation of Regional Phases Crossing the U.S.S.R.

Our understanding of the propagation of regional phases in the interior of the U.S.S.R. has been hampered by the lack of in-country seismic data. Although some information on regional phases from earthquakes in Russia is now available, no similar information exists for underground nuclear explosions except that recorded at stations outside the U.S.S.R. However, the usefulness of the latter data is itself limited because of the lack of correlative earthquake data with sources near the explosion sites and our limited understanding of how regional phase propagation is affected by geologic structure along the path, particularly for paths crossing the tectonically complex regions of Russia's southern and eastern borders.

In this description we will be concerned with the four regional phases which have received the most attention in the

literature: P_n, P_g, L_g and to a lesser extent S_n. Probably the most abundant type of information available on these phases is velocity of propagation. This type of information comes from a variety of sources including single and multiple station observations of earthquakes at regional distances (cf. Båth, 1954, 1957, 1959; Pec, 1961; Nersesov and Rautian, 1964; Gupta, et al., 1980) as well as refraction surveys (for P_n and P_g) with large spread lengths such as those encountered in Deep Seismic Sounding studies which have been conducted in many areas of the U.S.S.R. (cf. Volvovsky, 1973; Piwinskii, 1979). Figure 1 shows some typical regional phase travel time curves and velocities for southern Russia (Pamir-Lena River) developed by Nersesov and Rautian (1964) from earthquake data. Gupta, et al. (1980) show similar regional phase travel time curves for earthquakes and explosions in western Russia as observed at WWSSN stations surrounding the Soviet Union at distances from 5° to 30°. Their plot for shallow earthquakes is shown in Figure 2. For all the events studied the data indicate P_n or P velocities varying with distance from 8.26 to 8.49 km/sec for the distance range from 5° to 16°, from 9.8 to 10.38 km/sec for the distance range from 16° to 25° and from 12.19 to 12.96 km/sec for the distance range beyond 25°. Velocities for P_g were found to be between 5.52 and 5.66 km/sec, for S_n between 4.67 and 4.71 km/sec and for L_g from 3.49 to 3.57 km/sec. These velocities are in good agreement with those shown in Figure 1 for southern Russia and appear to be representative of regional phase velocities found throughout most of the Soviet Union.

More important to the discrimination problem are the amplitudes and attenuation of the regional phases. The most abundant published data on regional phase amplitudes in the U.S.S.R. appears to be that regarding L_g; some information is available on P_n and P_g but very little dealing with S_n. Piwinskii and Springer (1978) summarized the observations of

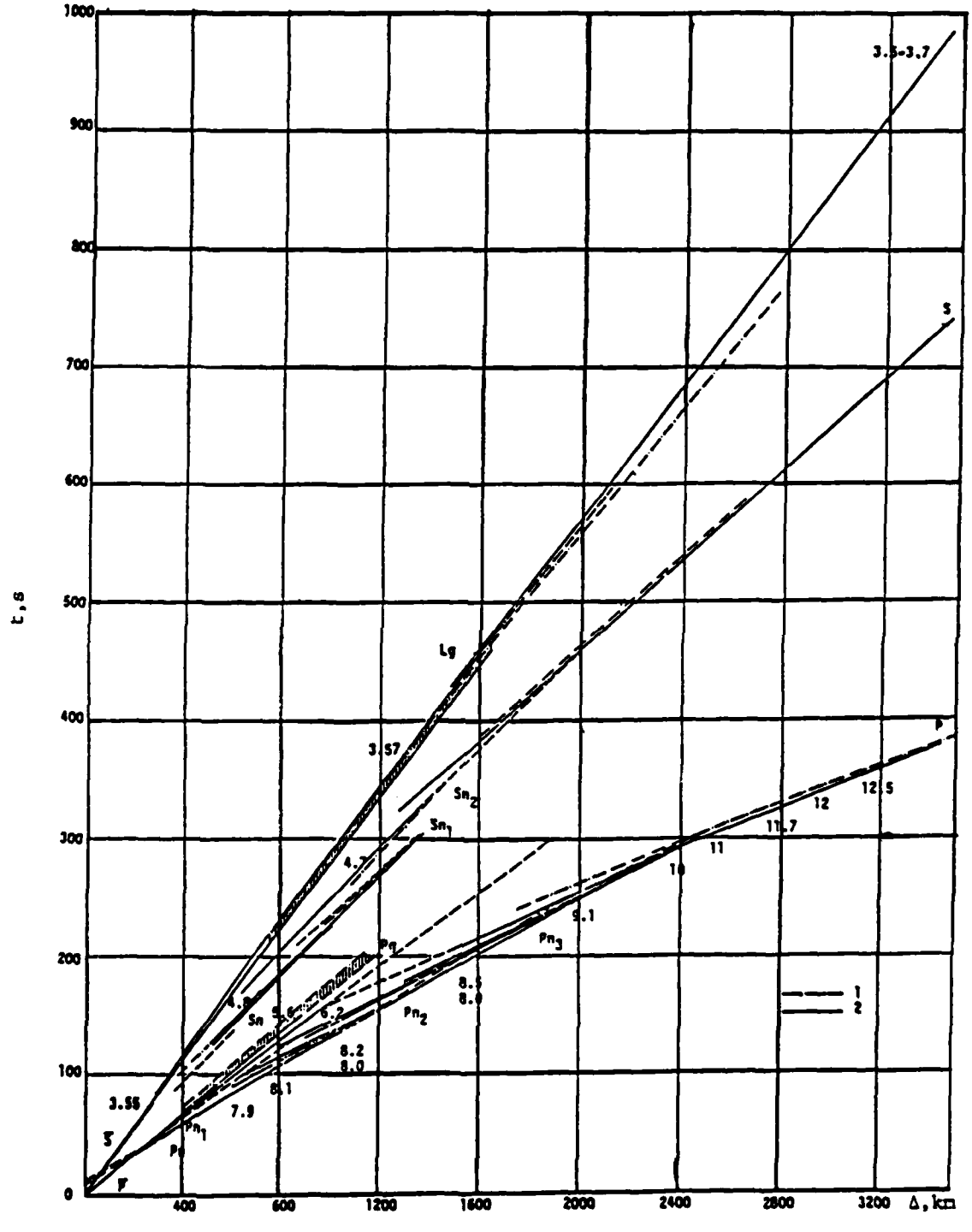

Figure 1. Regional phase travel times in southern Russia.

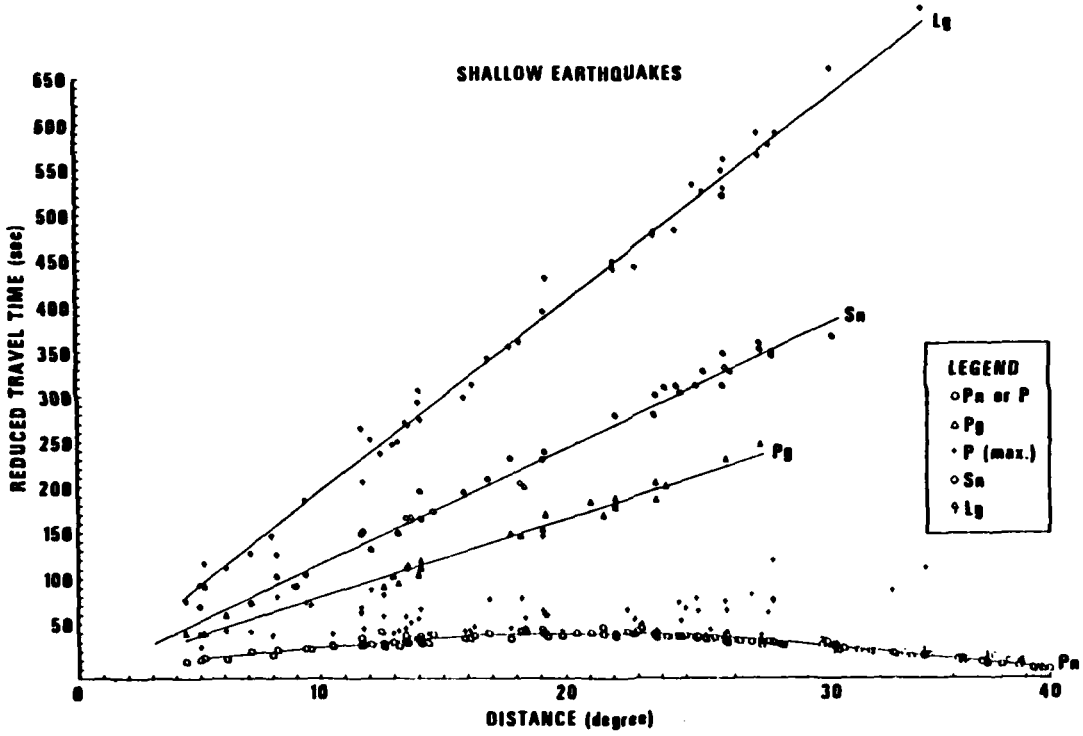

Figure 2. Reduced travel time curves for regional phases from Russian events recorded at WWSSN stations (after Gupta, et al., 1980).

several authors (viz. Båth, 1954, 1957, 1959; Payo, 1960; Utsu, 1958, 1960; Pec, 1961, 1962; Savarensky and Valdner, 1960; Sikharulidze, 1963; Ruzaikin, et al., 1977; Pshenikov, 1961; Valdner and Savarensky, 1961; and Rijikova, 1966) regarding the propagation of L_g phases across Europe and Asia. Although the data reported are for the most part qualitative, they do provide a general framework for understanding the efficiency of L_g propagation in these areas. Taken as a whole, the data suggest that L_g propagates efficiently throughout the platform areas and older fold systems of Asia and Europe (cf. Figure 3). The younger fold belts of the Alpine-Himalayan system and regions of oceanic crust produce erratic propagation or act to completely block transmission.

The study by Ruzaikin, et al. (1977) appears to have particular significance to assessing the potential value of L_g from events in south-central Russia recorded at regional distances to the south. Figure 4 shows their qualitative assessment of L_g from events throughout southern Asia recorded at two stations in southern Russia. Darker circles indicate that the earthquakes at those epicenters produced weak or no L_g at the recording stations shown as triangles. The poor L_g propagation from events to the south is attributed to strong attenuation or interruption of the wave guide in the Himalayan fold system or Tibetan Plateau (cf. Figure 3). Using reciprocity it may be possible to infer that events from the Soviet nuclear testing area in east Kazakh would be expected to produce, at best, weak L_g phases at recording stations near the darker circles.

Studies by Gupta, et al. (1980) were also in agreement with these findings. They reported on the efficiency of L_g propagation in southern Asia to stations at Kabul, Afghanistan and Meshed, Iran. Their findings are summarized in Figure 5. Clear L_g phases were found for nearly all paths from events north and northeast of the stations to ranges of 30°. However,

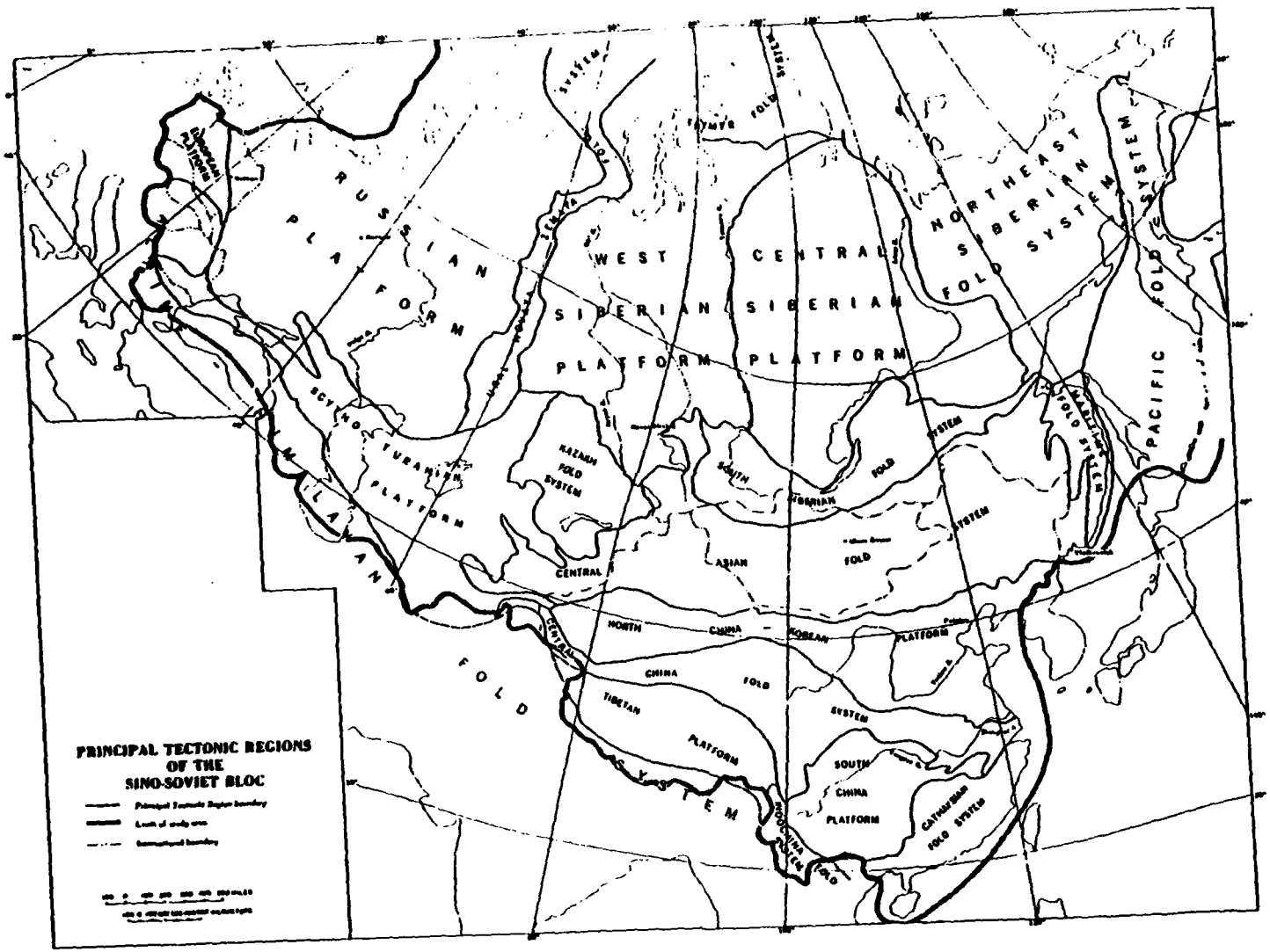

Figure 3. Tectonic subdivision of Asia.

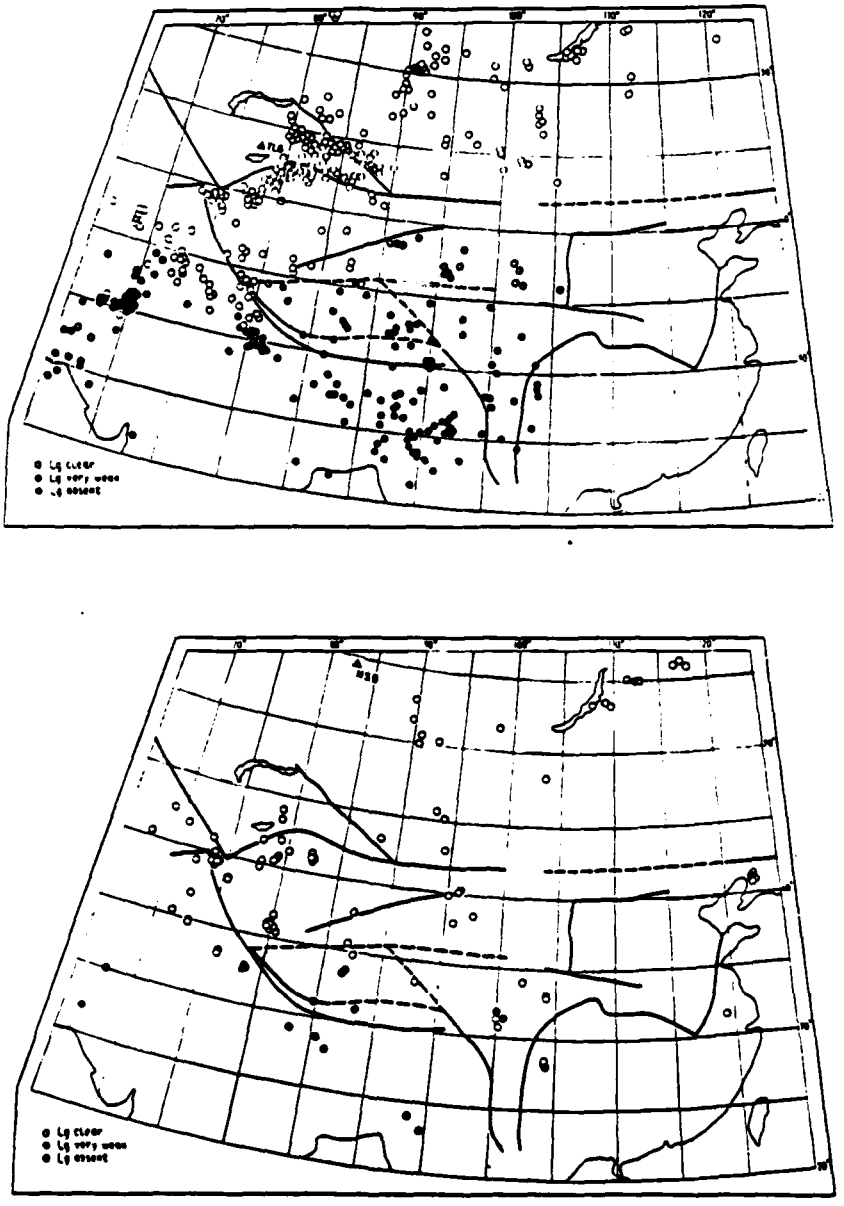

Figure 4. Efficiency of L_g propagation in the vicinity of Russia's southern border region. Earthquake epicenters indicated by circles; stations by triangles (after Ruzaikin, et al., 1977).

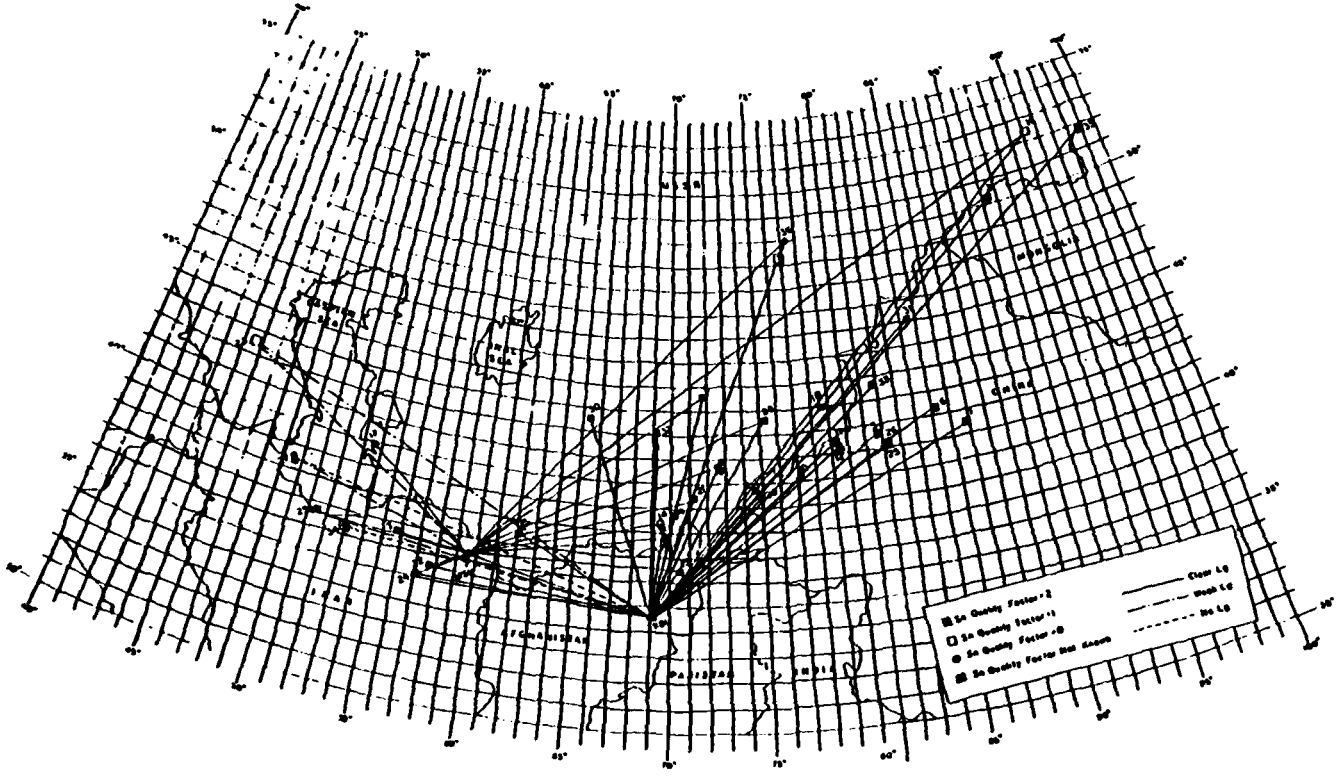

Figure 5. Efficiency of L_g propagation in Southern Asia for events recorded at Kabul and Meshed (after Gupta, et al., 1980).

for paths crossing the southern Caspian Sea and along the Himalayan-Alpine fold belt, coincident with Russia's southern border, behavior of the L_g phase was more erratic with frequent cases of weak or no phase recorded.

Similar qualitative information on the propagation efficiency of other regional phases is not generally available. However, considering that L_g and P_g phases are commonly associated with the presence of a granitic layer in continental type crust, the factors affecting L_g attenuation or interruption of the wave guide might be expected to similarly affect P_g. Although thickening of the crust under the Himalayas could also affect P_n and S_n phases, the attenuation would not necessarily be expected to be as severe as that for L_g and P_g.

More specific information on regional phase amplitudes and attenuation from events recorded at seismic stations within the U.S.S.R. has been published for some areas. Figure 6 shows amplitude attenuation curves for L_g, P_g, P_n and P phases observed along a line of stations in southern Russia from earthquakes in the Pamir Mountains (top) and Baikal area (bottom) (cf. Nersesov and Rautian, 1964). In general, P_g and L_g are seen to exhibit similar attenuation behavior with distance. The L_g amplitudes are larger than those of any of the P phases out to a distance range of 2500 km where they are more severely attenuated. It is also noteworthy that P_g data are not reported beyond 1200 km; at that distance their amplitudes become about the same level as the other P phases. The attenuation of P_n phases particularly at shorter distances appear more erratic.

Nuttli (1980, 1981) has recently published more detailed data on L_g attenuation from Russian events recorded at seismic stations outside the U.S.S.R. In his analysis, Nuttli has calculated an effective attenuation rate expressed in terms of a specific quality factor Q_0 for several nuclear explosions and some earthquakes in Russia observed along paths to the northeast

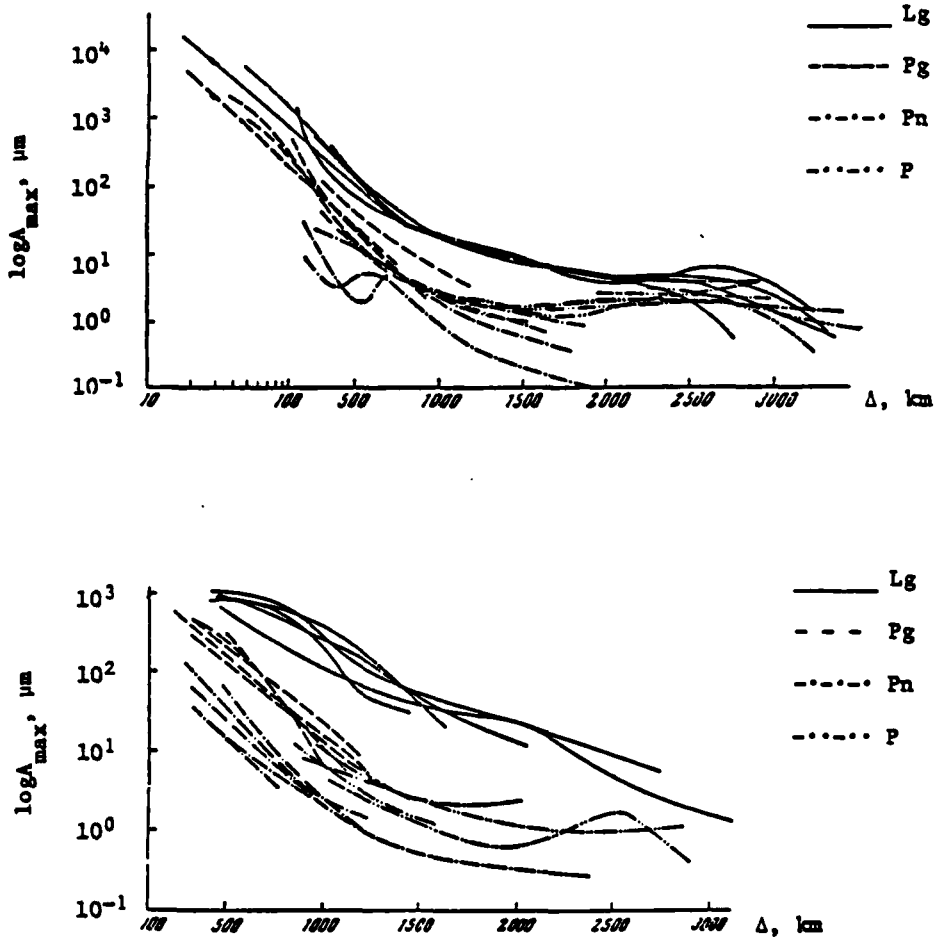

Figure 6. Attenuation of regional phase amplitudes across southern Russia from earthquake sources in the Pamir Mountain region (top) and Baikal area (bottom).

and south. Although some questions still exist regarding the reliability of the single station techniques used by Nuttli to estimate attenuation in this study, the results are in general agreement with previously cited findings. These results are indicated in Figures 7 through 10. Referring again to Figure 3, the data indicate high Q (low attenuation) across the platform regions but low Q (high attenuation) over most paths to the south into Iran and Afghanistan. However, some of the paths to the south crossing the Himalayan-Alpine fold belt appear to have higher than expected Q estimates. This is particularly notable for the east Kazakh explosions shown in Figure 10. Here the Q_0 estimates suggest attenuation levels intermediate between those of the eastern and western United States. For purposes of comparison, the Q_0 for one hertz L_g waves is estimated as 1200 for the central United States, 900 for the eastern United States and 200 for the western United States. The findings of Figure 10 do not seem to be in agreement with the results of Ruzaikin, et al. (1977) shown above in Figure 4 which suggested nearly complete blockage of L_g along some of these paths.

2.1.3 Discrimination Using Regional Phases

With regard to their use in discrimination, much of the research on regional phases has focused on measurements of the relative excitation of the P_g and L_g phases. The possibility of differences in excitation level for earthquakes and explosions has evolved primarily from observations in the eastern United States. Blandford and Hartenberger (1978) suggested that the ratio of the maximum amplitude before S_n to the maximum amplitude after S_n, as measured on short period vertical instruments, was a good discriminant between earthquakes and explosions. Subsequent studies (e.g., Pomeroy, 1980; Gupta, et al., 1980; Gupta and Burnetti, 1981) have attempted to apply this technique to Russian events recorded

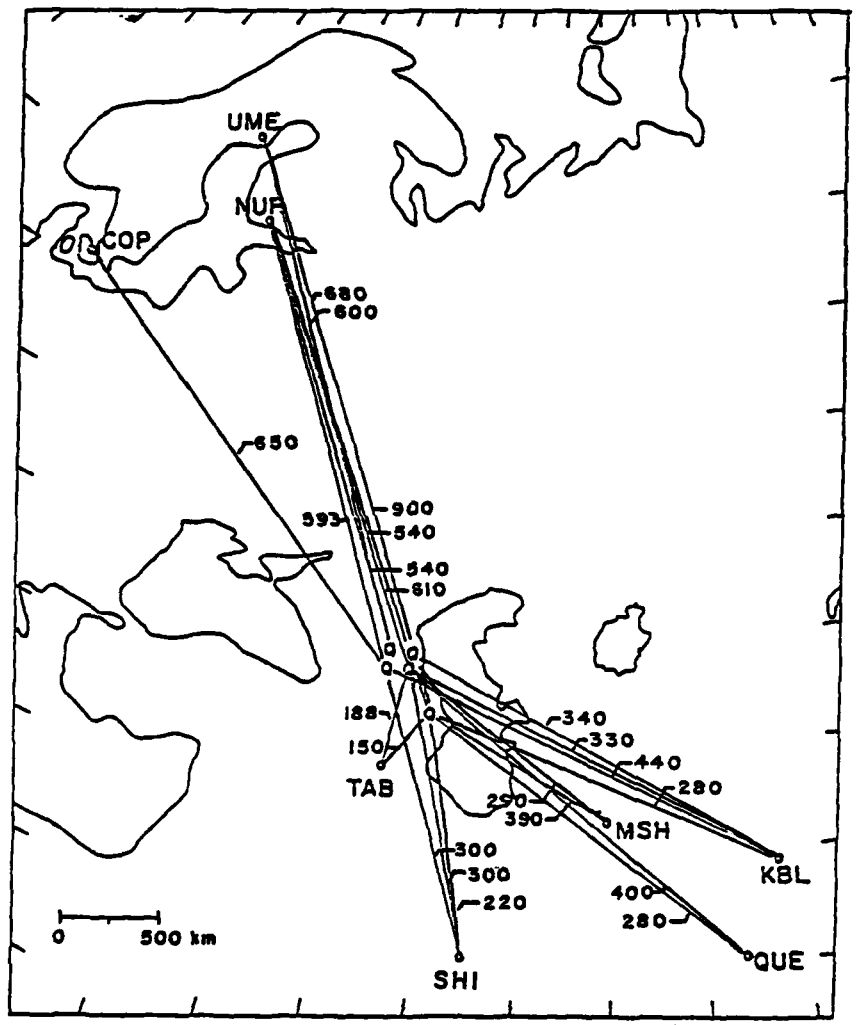

Figure 7. Attenuation of L_g phases in terms of Q_0 for paths in western and southern Asia from earthquakes in the eastern Caucasus. Event epicenters indicated by (Q); station locations by small circles.

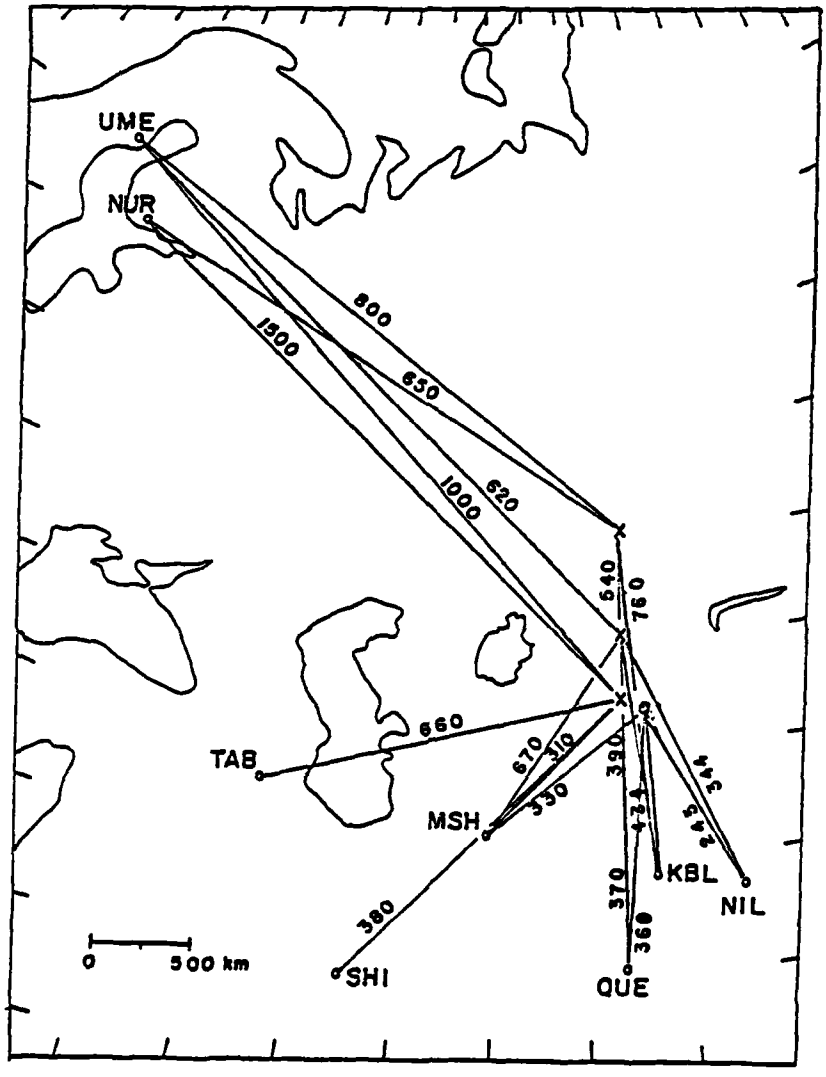

Figure 8. Attenuation of L_g phases in terms of Q_0 for paths in central and southern Asia from events in west Kazakh. Location of explosions indicated by (X); earthquake locations by (Q); station locations by small circles.

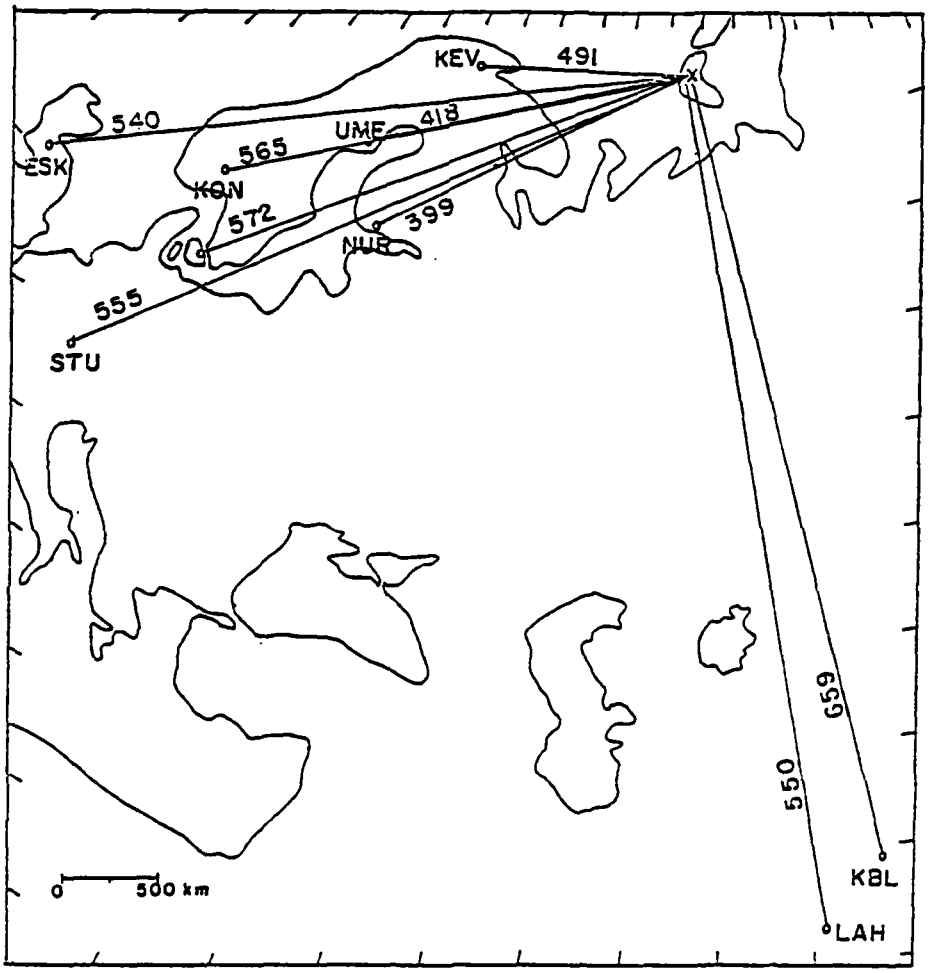

Figure 9. Attenuation of Lg phases in terms of Q_0 for paths in Central Asia and Northern Europe from explosions at Novaya Zemlya. Event epicenters indicated by (x); station locations by small circles (after Nuttli, 1980).

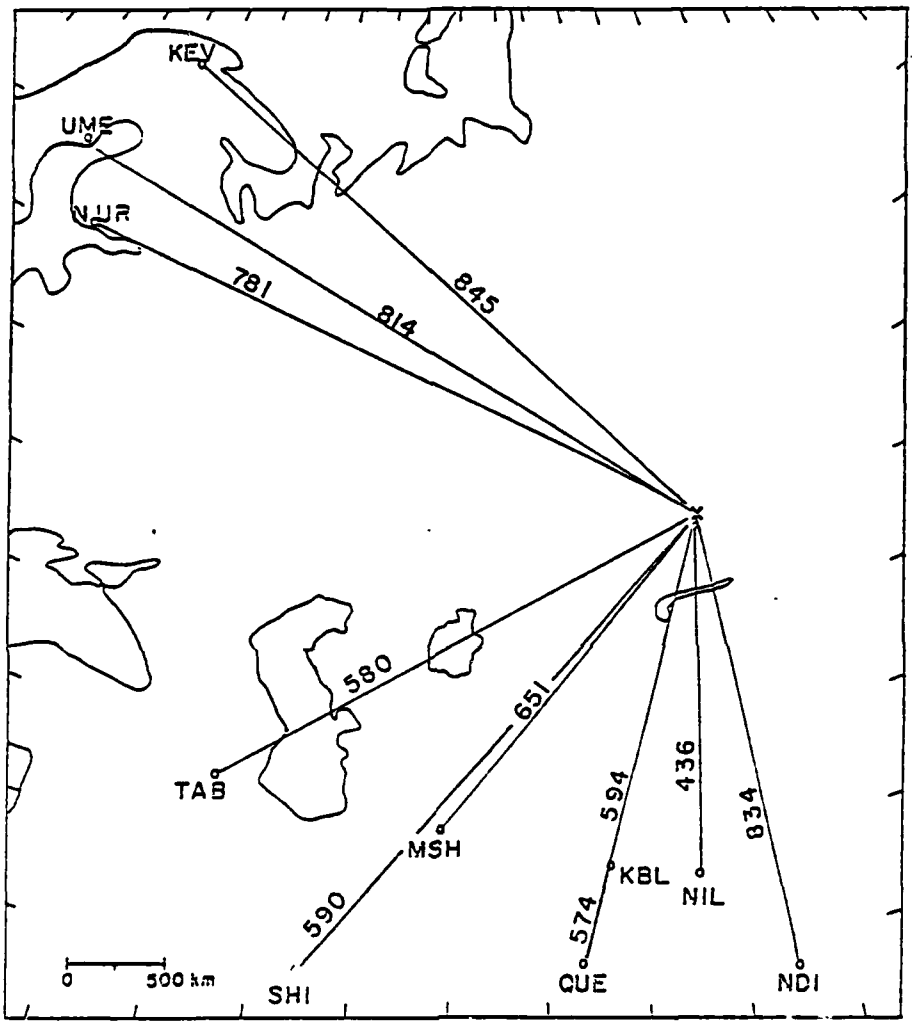

Figure 10. Attenuation of L_g phases in terms of Q_0 for paths in Central and Southern Asia from explosions in east Kazakh. Event epicenters indicated by (x); station locations by small circles (after Nuttli, 1980).

outside the country. In these cases, the maximum vertical amplitude after S_n has generally been interpreted to correspond to L_g while that prior to S_n is usually attributed to P_g as suggested by Figure 6 above. Pomeroy (1980) shows peak L_g versus maximum P wave amplitudes for earthquakes and explosions in central and western Russia (cf. Figure 11). In the central U.S.S.R. the L_g to P wave amplitude ratios are generally less than one for explosions and greater than one for earthquakes. Although there is considerable scatter in the explosion data, the results appear to offer some hope for use of such measurements in discrimination. The results for the western U.S.S.R. are not so promising. Both the earthquake and explosion data show a high degree of scatter and there does not appear to be much consistency with regard to L_g to P amplitude ratios being less than or greater than one. Pomeroy has not identified propagation paths for individual data points so it is unclear to what degree attenuation differences might be contributing to the observed scatter. Gupta and Burnetti (1981) compared the maximum amplitude prior to S_n (maximum P) and maximum amplitude after S_n (generally attributed to L_g) and also the maximum amplitude in the P_n window to the maximum amplitude in the L_g window for events in the southern U.S.S.R. recorded at Kabul and Meshed (cf. Figure 12). Although they found some separation between the mean trends of the data for the earthquakes and explosions, they show considerable scatter for individual data points. It seems clear from the available peak amplitude data, such as that described here, that some method for reducing the scatter, possibly by corrections for attenuation or source effects, is needed if such measurements are to evolve into a reliable discrimination tool.

Pomeroy (1979, 1980), based on consideration of the excitation characteristics of higher mode surface waves, hypothesized that the peak of the L_g motion could be expected

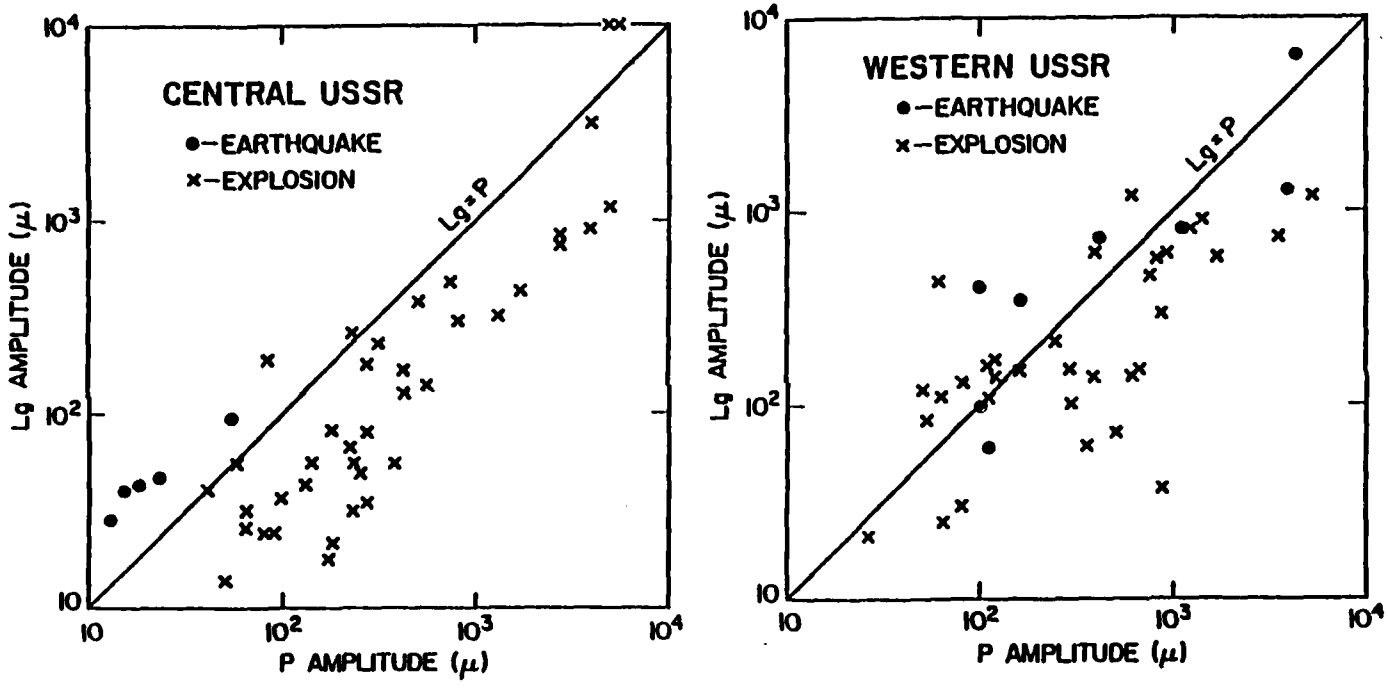

Figure 11. Comparison of peak L_g and maximum P amplitude measurements for events in the U.S.S.R. recorded outside the country.

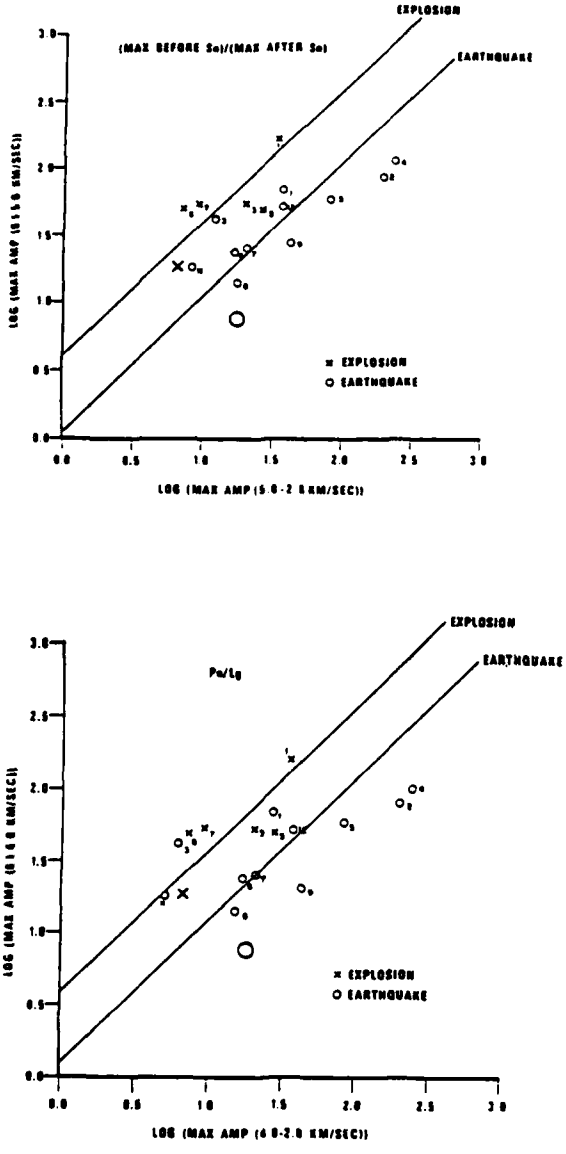

Figure 12. Comparison of peak amplitudes before and after S_n (top) and in the P_n and L_g windows (bottom) for explosions and earthquakes in Southern Russia recorded at Kabul (smaller symbols) and Meshed (after Gupta and Burnetti, 1981).

to have a lower group velocity for shallow events than for deep events. Thus, assuming that explosions are generally somewhat shallower than earthquakes, the group velocity corresponding to the peak L_g amplitude in explosions would be expected to be lower than that for earthquakes from the same area. Pomeroy has tested this hypothesis using two approaches: one based on a single measurement of the velocity corresponding to the peak L_g motion and the other based on a computation of energy in a high and low velocity window of the L_g motion. Pomeroy's results for the eastern United States appear to agree with the proposed hypothesis; however, the application to the U.S.S.R. is less convincing. Figure 13 shows the group velocities determined from peak motions for events in the U.S.S.R. The relatively small earthquake sample is seen to have group velocity values both above and below the bulk of the explosion data. Additional refinements using data with common source regions and transmission paths show somewhat more optimistic results; but more complete testing using a larger earthquake sample is needed to assess this technique.

2.1.4 Summary

Several observations can be made regarding regional phases from Russian events:

- Propagation velocities associated with regional phases in the Soviet Union are about 7.9 to 8.3 km/sec for P_n (somewhat higher at larger distances), 5.6 to 6.0 km/sec for P_g, about 4.7 km/sec for S_n and about 3.5 km/sec for L_g.
- Regional phases, and in particular L_g, appear to propagate efficiently along most paths within the Soviet Union – i.e., platform areas and older fold systems.

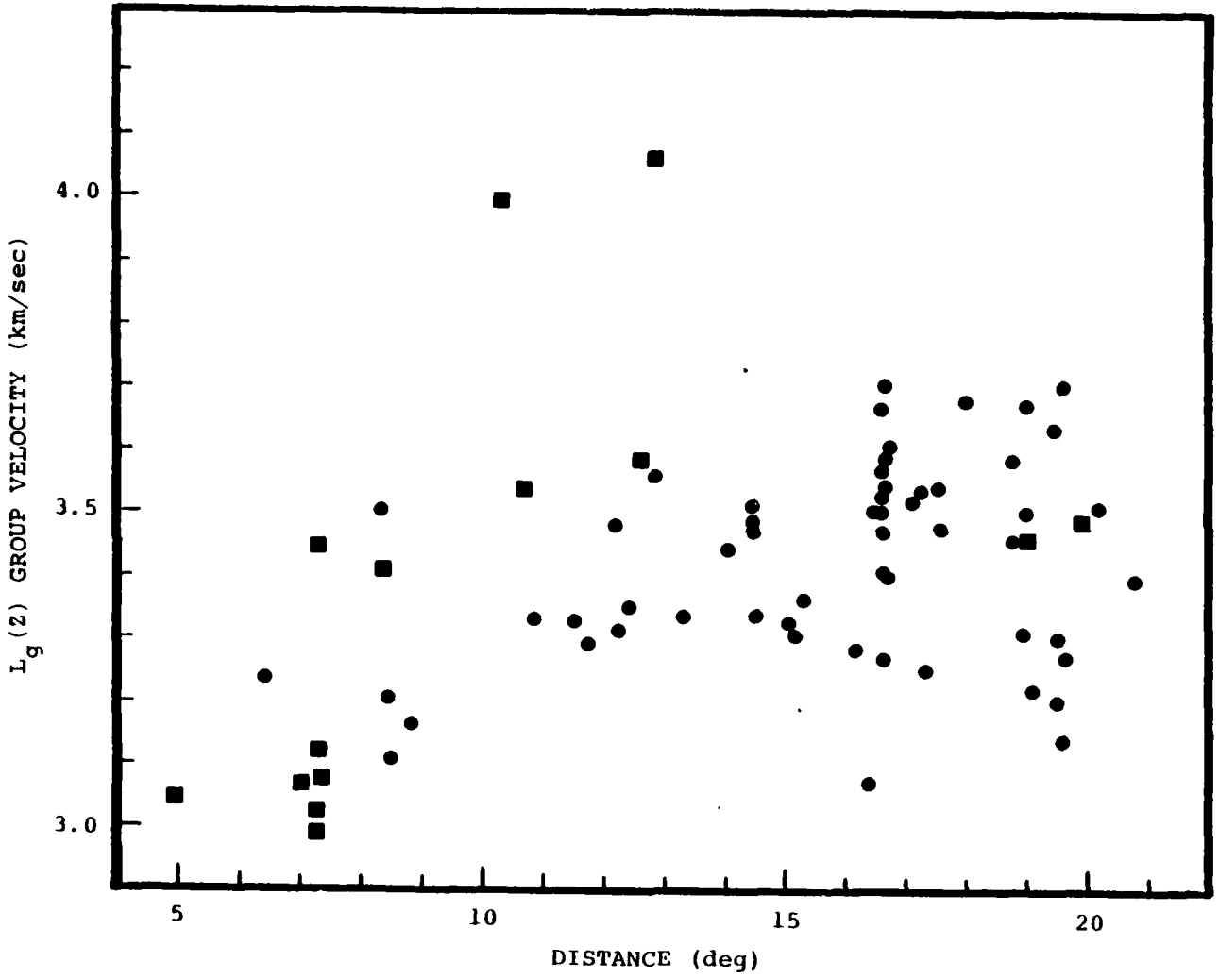

Figure 13. Group velocities corresponding to peak L_g amplitudes for U.S.S.R. explosions (circles) and earthquakes (squares).

- The regional phases L_g, and probably P_g, do not propagate efficiently across the region to the south of Russia – i.e., the younger fold system of the Alpine-Himalayan orogeny.

- Data from at least some areas of the U.S.S.R. indicate that L_g produces signal amplitudes from earthquakes larger than any P phases out to distances of 2500 km or so. P_g phases from the same area are not reported beyond about 1200 km where their amplitude level is equivalent to that of other P phases.

- The effective attenuation for one hertz L_g waves in the platform and older fold regions of central Russia is low, approximately equivalent to that in the eastern United States. Attenuation in the southern border region is high, more like values measured in the western United States.

- Discriminants based on measures of peak amplitudes of L_g, P_g and P_n show some evidence of separation between the means of earthquakes and explosion sets, but the scatter in the data does not currently permit reliable discrimination.

- Discrimination techniques based on L_g group velocity show separation between earthquake and explosion data in some tectonic environments but not others and need further refinement and testing.

2.2 COMPARISON OF REGIONAL PHASES FROM WESTERN UNITED STATES EXPLOSIONS AND EARTHQUAKES

2.2.1 Introduction

There has been a great deal of interest in the potential use of regional phase measurements as discriminants between earthquakes and underground nuclear explosions. Several studies (e.g., Blandford and Hartenberger, 1978; Blandford, et al., 1980; Pomeroy and Chen, 1980; Nuttli, 1981; Gupta and Burnetti,

1981) have focused on the propagation characteristics and relative excitation of the L_g and P_g phases mainly because, in many tectonic environments, they are the strongest regional phases and therefore the most likely to produce measurable signals for even small events. The potential of regional phases, and in particular the L_g and P_g phases, has remained indeterminant largely because a definitive data base with earthquake and explosion sources in close proximity has not been assembled and theory has not developed to the point of permitting extrapolation of experience between different source and propagation environments. In the following, we focus on the development of a more definitive data base to better establish excitation differences for regional phases from earthquakes and underground nuclear explosions.

2.2.2 Analysis of NTS Data

Blandford and Klouda (1980) recently reported on the L_g, P_g and P_n phases from a large group of NTS underground nuclear explosions recorded at the Tonto Forest Observatory (TFO) about 500 km away. Using rather simple peak-amplitude, time domain measurements for velocity windows corresponding to the appropriate regional phases, they developed relations between L_g, P_g and P_n amplitudes (vertical component) for the NTS explosions. Their results for P_g and L_g are shown in Figure 14 where the slope of the linear regression was constrained to one and the dashed lines represent 2σ error bounds. The equation of the line is $\log A_{P_g} = \log A_{L_g} + 0.1$.

In the current program, Bennett and Murphy (1980) studied a sample of 21 earthquakes covering a body-wave magnitude range from 3.3 to 4.6 which occurred within about one degree of NTS (cf. Figure 15) and were recorded at TFO. To avoid the ambiguity of collapse events or unannounced tests, we excluded all events located on the test site except for two events known to be earthquakes near Massachusetts Mountain ($m_b \approx 4.3$) and near

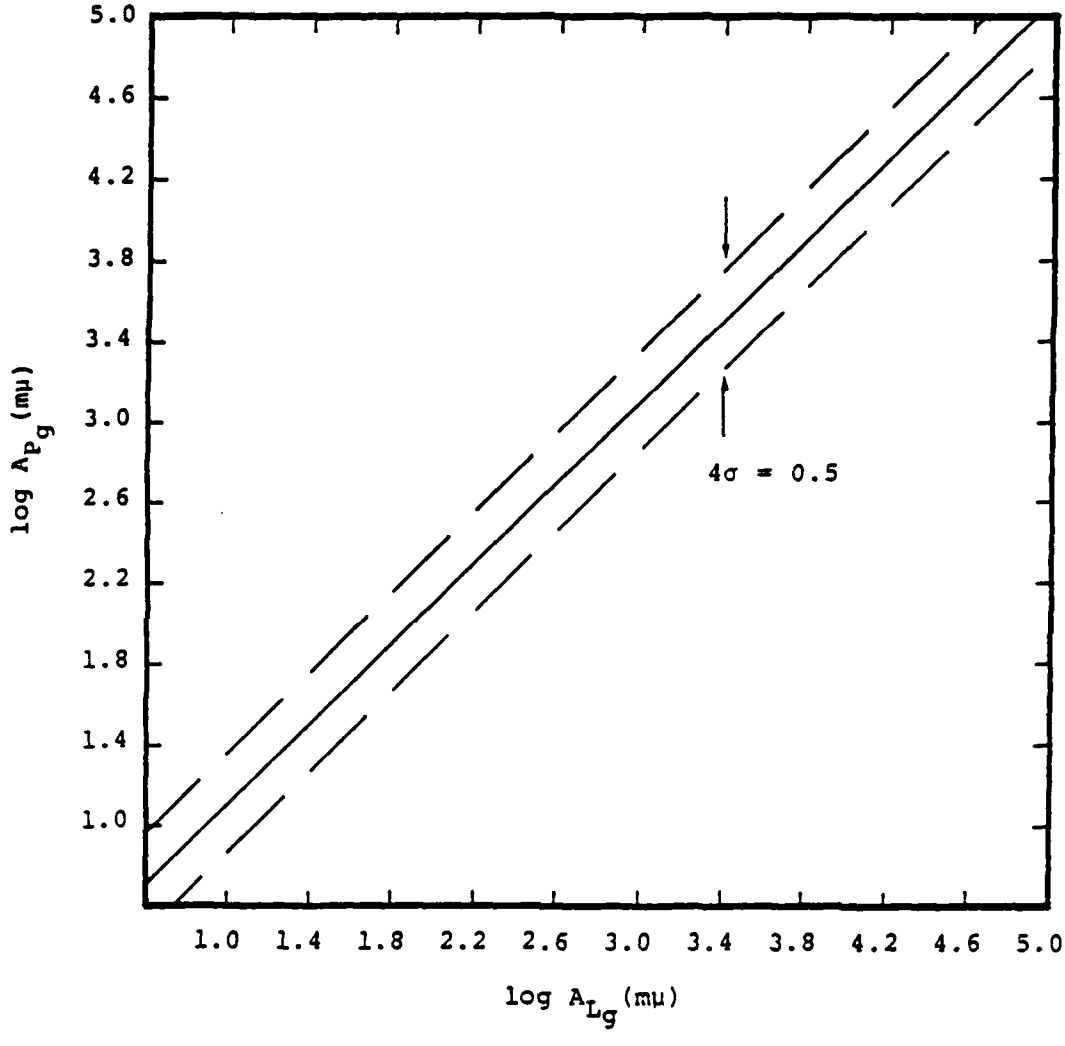

Figure 14. Linear regression relating P_g and L_g amplitudes for explosions at NTS developed by Blandford and Klouda (1980).

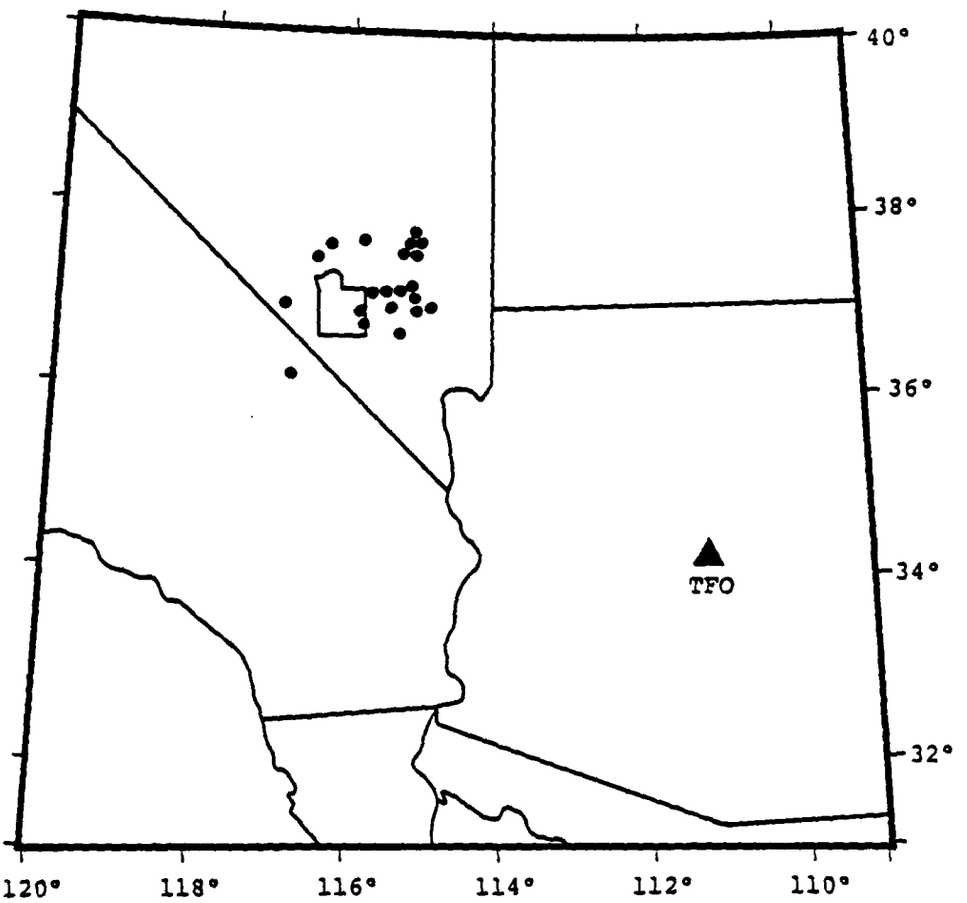

Figure 15. Earthquake sample from the vicinity of NTS with regional phases recorded at TFO. Circles indicate epicenters; triangle is the station location.

Ranger Mountain ($m_b \approx 4.2$). We followed a procedure like that used by Blandford and Klouda (1980) and measured peak amplitudes in time windows corresponding to the propagation velocities of the expected regional phases. The necessity of such a procedure is illustrated in Figure 16 which shows a typical time history. The maximum amplitudes are somewhat lacking in character and in many cases are nearly indistinguishable from the surrounding wave trains. Figure 17 summarizes our results for P_g and L_g phases from the earthquakes near NTS. The linear regression was again constrained to have a slope of one resulting in the relation:

$$\log A_{P_g} = \log A_{L_g} - 0.1$$

for the earthquakes. As can be seen in the figure, most of the earthquake data points fall below the mean explosion line. However, the scatter in the earthquake data is so large that the 2σ error bounds envelop the mean explosion line and, in fact, most of the explosion data. For the two earthquakes at NTS, the Massachusetts Mountain earthquake data point falls well below the mean earthquake line and hence discriminates very well from the explosion data. On the other hand, the Ranger Mountain earthquake data point falls very close to the mean explosion line and would not discriminate.

Similar measurements of the P_n and L_g phases for the earthquakes and a sample of the explosions in the magnitude range from 3.5 to 4.8 is shown in Figure 18. The data appear to be intermingled and offer little promise for their use in discrimination.

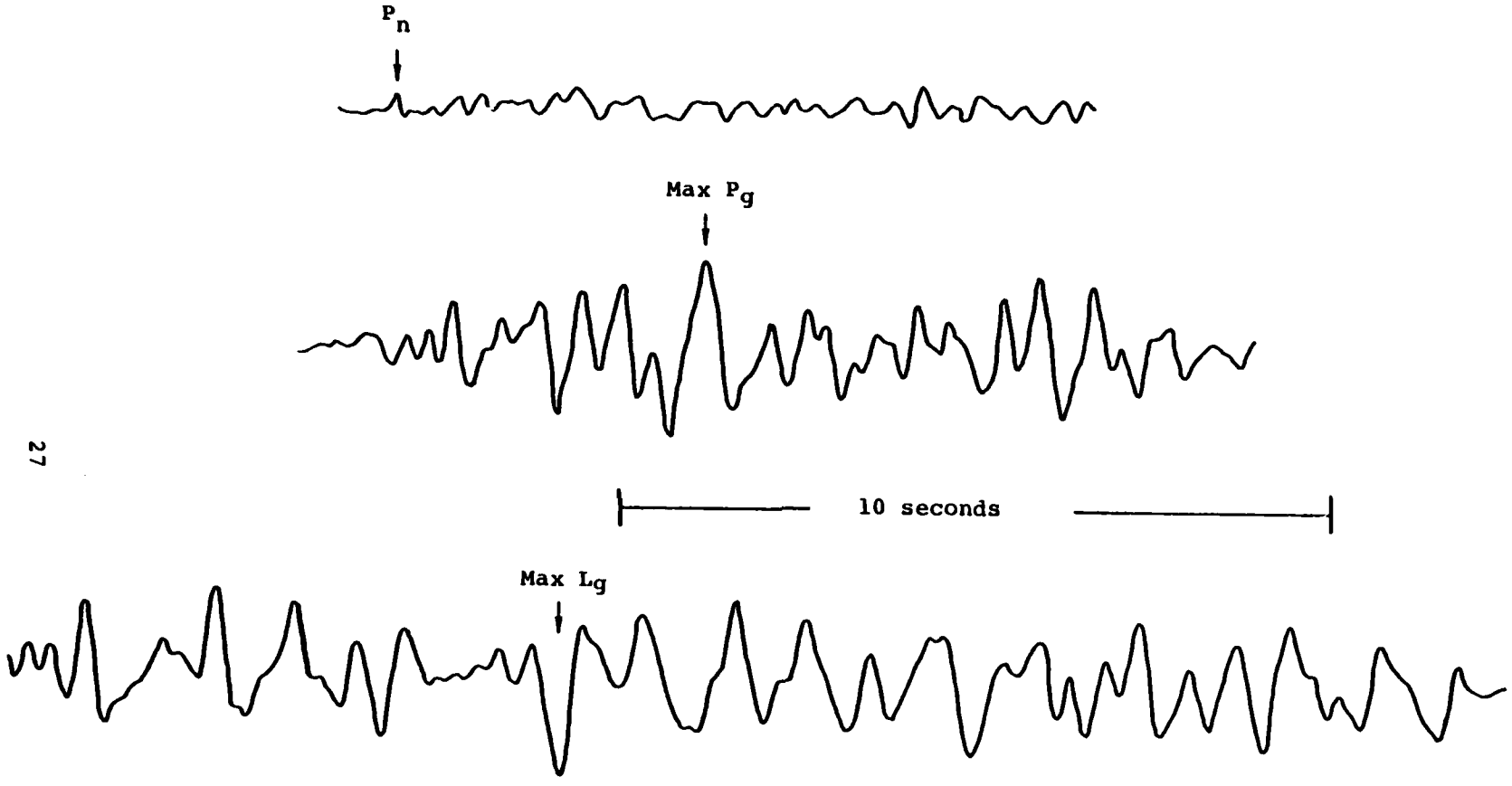

Figure 16. Typical record of regional phases P_n, P_g and L_g recorded at TFO from an earthquake in the vicinity of NTS.

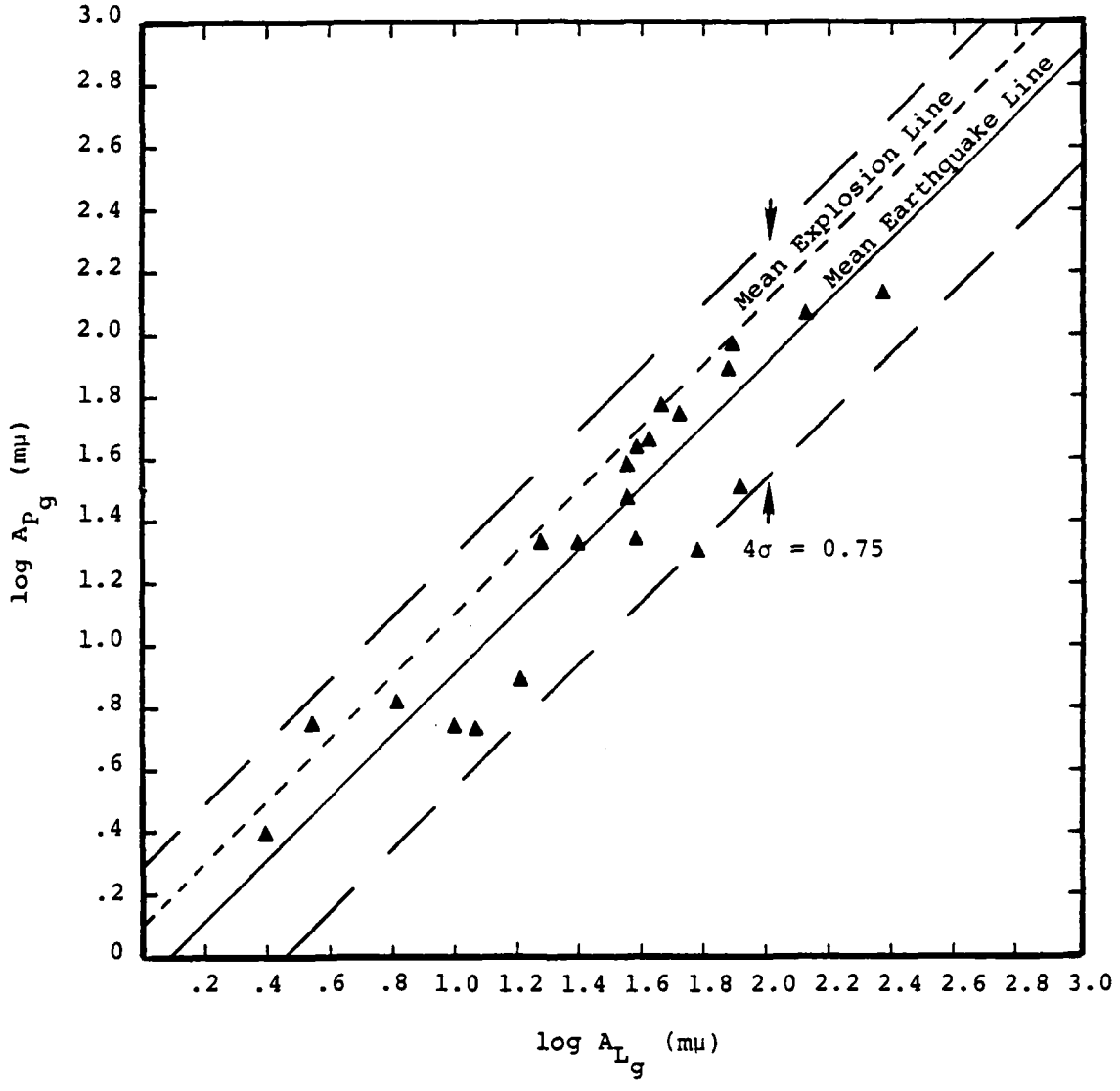

Figure 17. Comparison of P_g and L_g amplitudes recorded at TFO from earthquakes near NTS. Triangles indicate data points and the solid line is a regression line through the data.

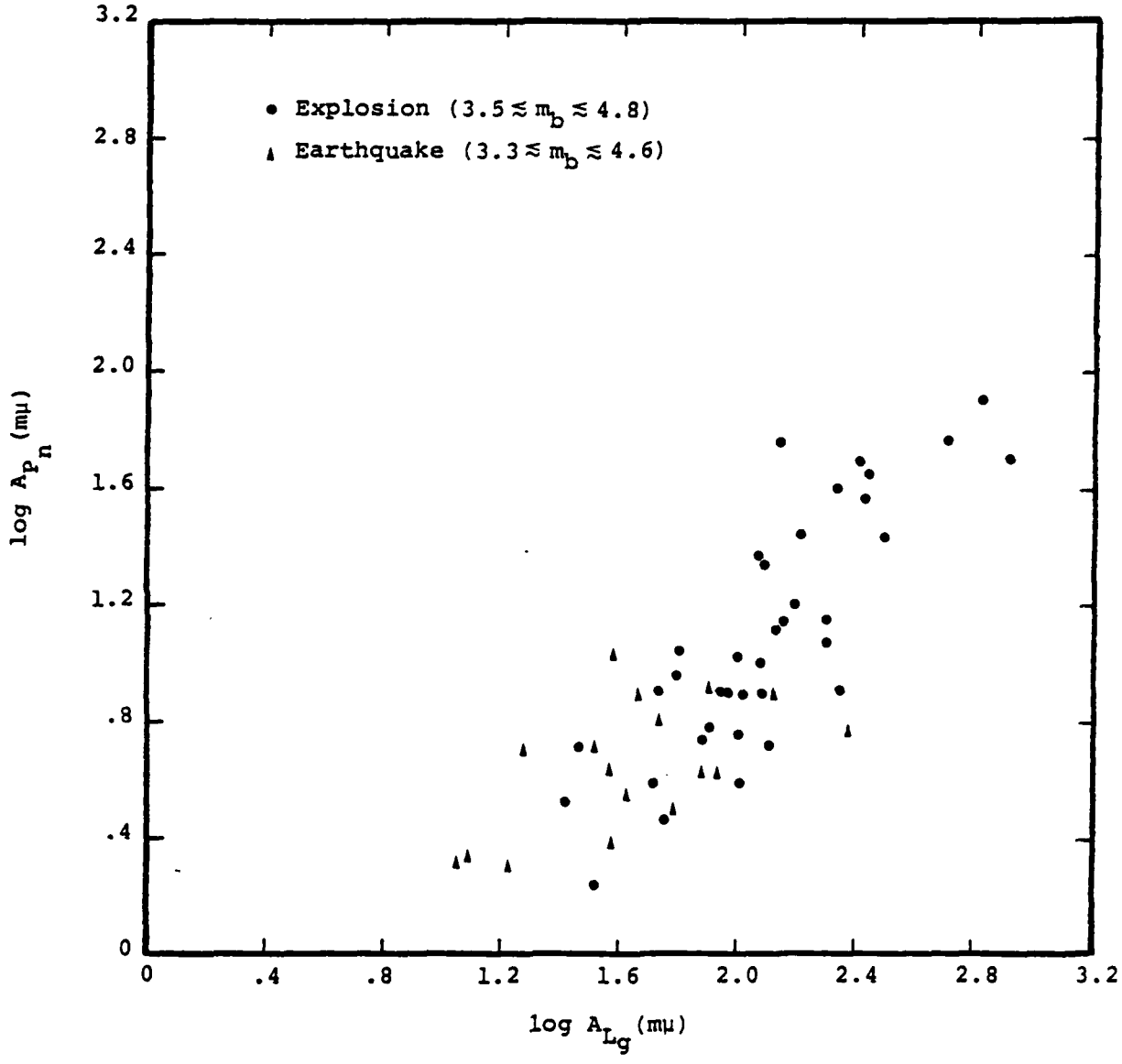

Figure 18. Comparison of P_n and L_g amplitudes recorded at TFO from earthquakes near NTS.

2.2.3 Factors Affecting the Discriminants

Among the factors which have been thought to affect the amplitudes of regional phases, and hence to be a source of the observed scatter, are source depth, regional propagation path and recording site response. We will say more about the source-depth effect in Section 2.3. In our study of the NTS earthquake data we attempted to minimize any differences in regional propagation path and recording site by using only a single station and limiting the earthquakes to a relatively narrow band of azimuths relative to the recording site at TFO. In a second part of the study we attempted to investigate these factors using earthquakes mainly in California (cf. Figure 19) recorded by short-period instruments in three different areas of NTS.

We made measurements of the P_g and L_g amplitudes like those which we made above for the TFO recordings. The results are summarized in Figure 20. Different symbols correspond to different recording sites on NTS. For each earthquake an observation was generally available for Climax Stock and for either Pahute Mesa or Yucca Flats. The Climax Stock observations are confined mainly to lower values while Pahute Mesa and Yucca Flats data cluster at higher values suggesting that the Pahute Mesa and Yucca Flats sites tend to amplify the P_g and L_g phases relative to Climax Stock. A similar result was reported by Barker, et al. (1980) using the same data base. It is also interesting to note that the trend in the data remains close to a slope of one. It is unclear whether differences in source excitation or attenuation are responsible for the slightly lower intercept of these data relative to the TFO mean lines.

2.2.4 Summary

Analysis of regional phases from earthquakes and explosions in the vicinity of NTS and from a supplemental set of

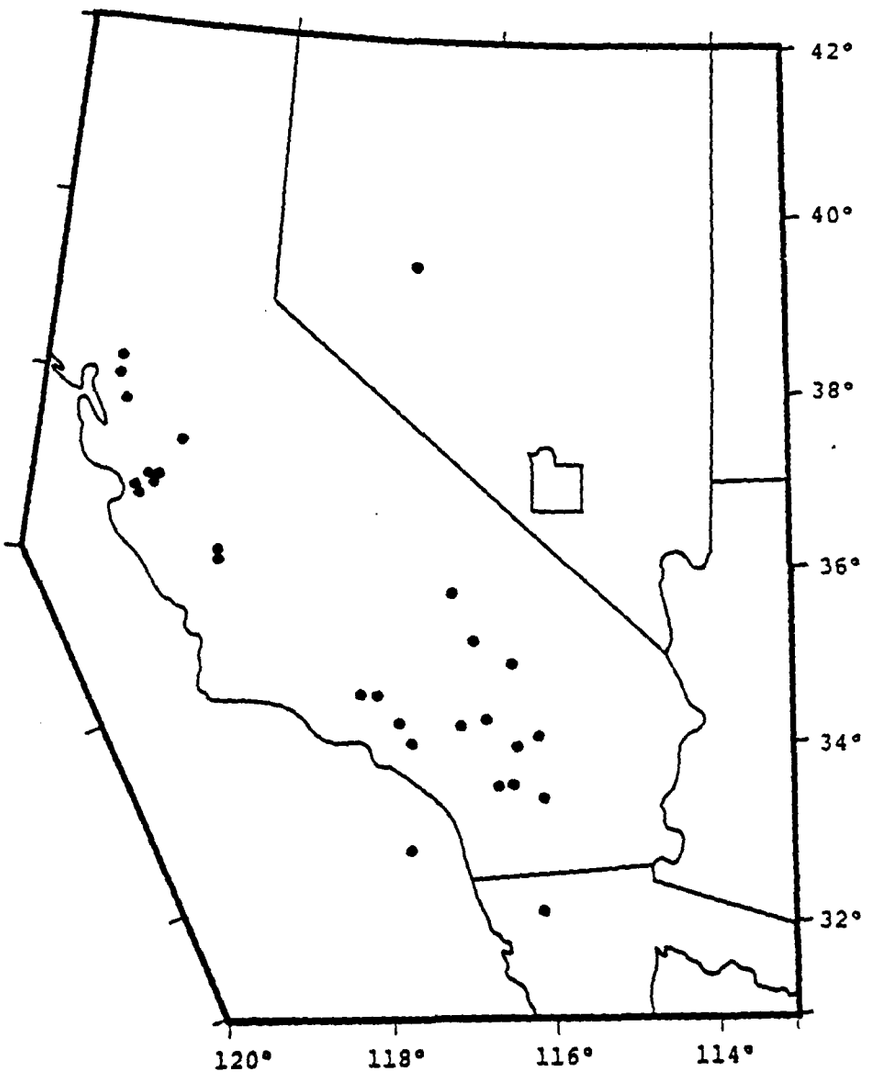

Figure 19. Earthquake sample recorded at NTS used in analysis of depth and recording site effects.

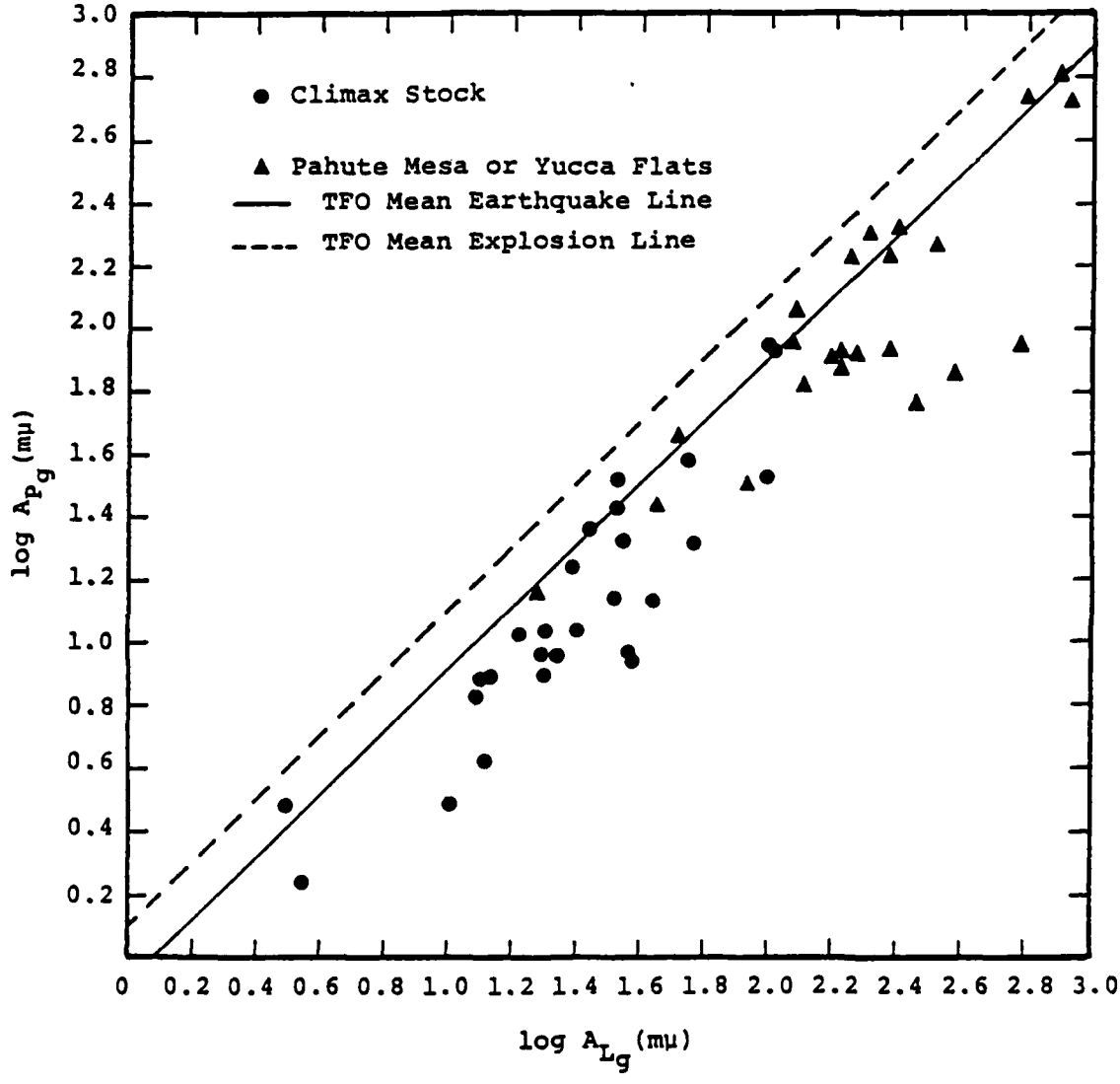

Figure 20. Comparison of P_g and L_g amplitudes from California earthquakes recorded at different locations on NTS.

California earthquakes recorded at NTS has led us to conclude that:

- The P_g to L_g amplitude ratios for earthquakes in the vicinity of NTS, based on simple peak motion measurements, average less than one.
- This observation contrasts with similar amplitude ratios measured for NTS underground nuclear tests which average more than one.
- The earthquake amplitude measurements show relatively large scatter which envelopes the explosion values and places in question the reliability of the discriminant.
- The relation between P_g and L_g amplitudes from earthquakes does not appear to be particularly sensitive to detailed differences in site response but may show some dependence on transmission path and focal depth (i.e., see following section).
- The indistinct character of many of the observed regional phases suggests that measurements other than simple peak amplitude observations may better represent signal strength in regional phase wave trains and may produce a better discriminant.

2.3 DEPENDENCE OF L_g EXCITATION ON SOURCE DEPTH

2.3.1 Introduction

As was noted in Section 2.2.3 above, one of the factors which can be expected to have an effect on the amplitudes of regional phases is source depth. This is especially true with

regard to L_g which is now generally recognized to correspond to the superposition of higher mode Love and Rayleigh surface waves which are known to have a pronounced dependence on focal depth. In particular, surface wave excitation is generally expected to decrease with increasing source depth and, since the amplitudes of regional P phases such as P_g and P_n are known to be relatively insensitive to focal depth, P/L_g ratios might be expected to increase with the depth of the source. This suggests that deeper earthquakes may have explosion-like P/L_g ratios, perhaps providing a partial explanation for the overlap in the explosion and earthquake data sets such as that shown in Figures 17 and 18. We have been investigating this issue using both the results of theoretical modeling and analyses of regional phase data recorded at NTS from a number of southern California earthquakes covering a representative range in focal depths.

2.3.2 Summary of Theoretical Modeling Results

The L_g phase is a high frequency wavetrain which arrives with a group velocity near 3.5 km/sec. It is observed on all three components of motion for both explosions and earthquakes and is often the dominant arrival on short period recordings in the regional distance range. As a result of its prominence, it has been the subject of numerous empirical investigations. However, attempts to synthesize this phase theoretically date back only a few years and, consequently, the analytical definition of the dependence of L_g excitation on variables such as source depth and crustal structure is the subject of ongoing research. Bache, et al. (1980) recently completed a study in which they attempted to theoretically synthesize vertical component L_g waveforms using superposition of Rayleigh modes in a plane-layered crustal model. The applicability of this proposed synthesis technique was assessed through comparisons with regional data measured in the eastern United States from the SALMON

explosion. Although these detailed comparisons are not entirely satisfactory at the present time, they do suggest that the theoretical model can explain the major features of the observed L_g phase and thus should be useful for the parametric evaluation of the dependence of L_g excitation on the model parameters.

In particular, with regard to the dependence of L_g excitation on focal depth, Bache, et al. (1980) have synthesized L_g wavetrains for point double couple earthquake sources at ten different depths (i.e. 1, 2, 4, 5, 6, 8, 11, 14, 15 and 25 km) in an approximate eastern United States crustal model. For this application, the seismic moment of the double couple was held fixed at 10^{25} dyne-cm and the source time history was taken to be a step function so that the source function has no characteristic corner frequency. Seismograms were computed for this source oriented to represent strike-slip, vertical dip-slip and 45° dip-slip faulting (i.e. the solutions for any other fault orientation can be obtained by linearly superposing solutions for these three basic orientations). It was found that there is little systematic dependence of the waveforms on depth, with the possible exception that the duration of the vertical dip-slip synthetics appears to decrease somewhat with increasing depth. However, the maximum amplitude of L_g does show a pronounced depth dependence. Figure 21 shows the theoretical L_g amplitudes (as seen on the output of a WWSSN short period instrument at a range of 1000 km) as a function of source depth for the three source orientations. The source locations are shown with respect to the adopted crustal model (shear wave velocity β, attenuation parameter Q) and, from this display, it appears that there is no evidence that the L_g amplitude depends on the layer in which the source is located. Thus, to first order, the depth dependence should be independent of the details of the crustal model. It can be seen that for both the strike-slip and 45° dip-slip sources the amplitude of

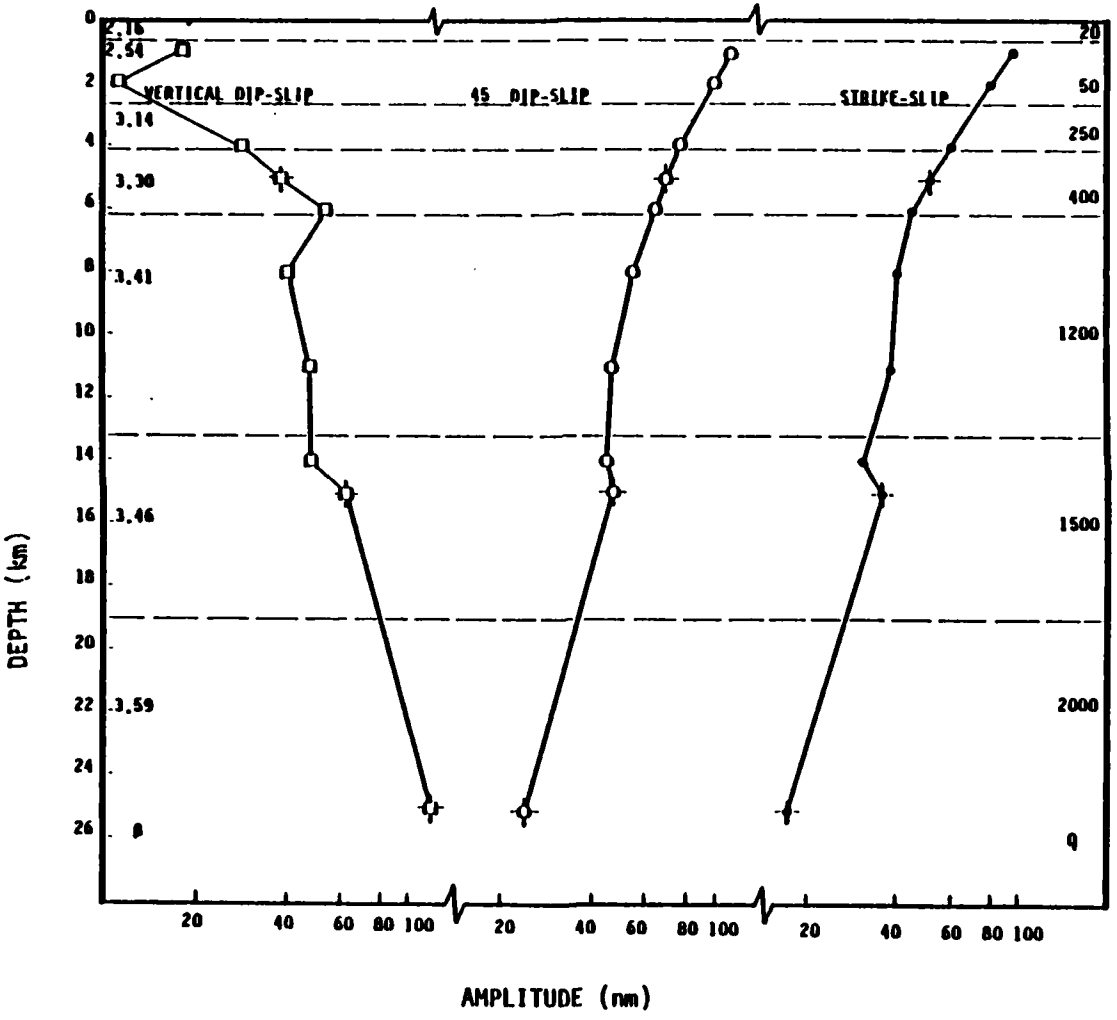

Figure 21. Dependence of L_g amplitude on source depth for three different double couple orientations.

L_g decreases with increasing source depth, as expected. Over the depth range from 1 to 25 km, the L_g amplitude is predicted to decrease by a factor of four to five for these two source orientations. However, the depth dependence of the L_g phase radiated from the vertical dip-slip source shows a more complicated pattern with the predicted amplitude actually increasing with depth over some ranges.

Thus, the L_g depth dependence predicted by available theoretical models depends on source orientation and it follows that although a decrease in L_g amplitude with depth can be expected in most cases, variations in focal mechanism may introduce considerable scatter.

2.3.3 Analysis of Southern California Earthquake Data

In parallel with the ongoing theoretical studies, we have also been analyzing recorded earthquake data in an attempt to empirically define the effects of focal depth on the P/L_g type regional discriminants. For this purpose we have selected a sample of 16 southern California earthquakes with focal depths (NEIS) ranging from 1 to 16 km. All of these events were recorded at the same temporary station located at Climax Stock on NTS. Thus, the propagation path and local receiver site effects should be approximately constant and should not mask any systematic effects of focal depth. The amplitudes of the various regional phases recorded at the Climax Stock station from these earthquakes have been read following the procedure described previously in Section 2.2.2 and Figure 22 shows the resulting P_g to L_g amplitude ratios plotted as a function of focal depth. It can be seen that although the data show considerable scatter, there does appear to be a tendency for the P_g/L_g ratio to increase with increasing focal depth, in qualitative agreement with the theoretical prediction for strike-slip faulting. More specifically, for the cluster of events near 6 km focal depth

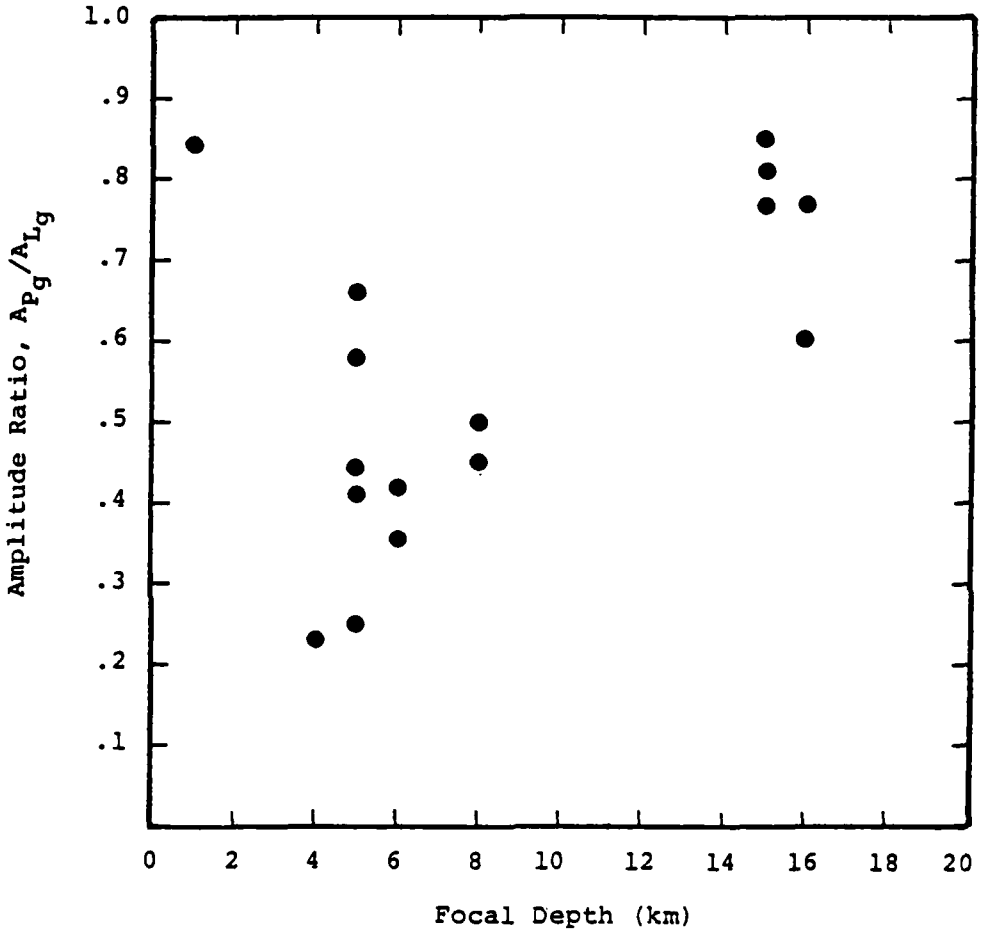

Figure 22. Dependence of P_g/L_g amplitude ratios on focal depths for Southern California earthquakes recorded at NTS.

the amplitude ratios average 0.4 to 0.5 while the data at 15 to 16 km focal depths show amplitude ratios of near 0.8.

2.3.4 Summary

Analyses of both the results of theoretical modeling and a limited sample of empirical data suggest that the excitation of the L_g phase generally decreases with increasing focal depth. In particular, the theoretical simulations and observed data both indicate about a factor of two reduction in L_g peak amplitude level for strike-slip sources over the depth range from about 5 to 15 km. This effect is larger than the average difference between earthquake and explosion L_g amplitude levels and tends to make deeper earthquakes look explosion-like with respect to the P/L_g discriminants. These preliminary conclusions are currently being tested against a larger sample of regional data recorded from Eurasian events.

2.4 DEVELOPMENT AND TESTING OF SPECTRAL DISCRIMINANTS

2.4.1 Introduction

In Sections 2.1 to 2.3, we emphasized the development of discrimination techniques based on time domain measurements (amplitude and period) of regional seismic phases. In this section we focus on spectral methods. In the following discussion we consider some preliminary results of the variable frequency magnitude (VFM) approach (Archambeau, et al., 1974) from a study of the SALMON explosion and Alabama earthquake pair. This work is designed to test the VFM discrimination approach for a closely located explosion-earthquake pair in the eastern United States, where relative attenuation effects are reduced and common stations are available. We conclude this section with a description of a signal analysis approach

which is expected to provide more accurate spectral measurements of discrimination parameters for isolated regional phases.

2.4.2 Preliminary Results for the SALMON Explosion and Alabama Earthquake Events

The SALMON and Alabama events were seismically recorded at many common LRSM stations. However, digital data for the Alabama earthquake earthquake are available at S^3 for only some stations common to SALMON. These data lie along a northeasterly line from the explosions and earthquake epicenters (Figure 23). Since the objective of the study is to look at detailed source spectral differences we need to account for path and receiver effects. This can be accomplished either experimentally by selecting common paths and receiver combinations or theoretically treat the problem using detailed knowledge of crust and upper mantle velocity and Q structures. The latter information is known generally but not in sufficient detail to adequately predict the desired effects. However, with the experimental approach path effects can be substantially negated by comparing data along common paths and equivalent distances. That is, the spectral difference observed should be due to only the source if path and receiver are the same. However, experimental realities prevent such ideal comparisons. For example, digital data are available at EUAL for the Alabama earthquake but not for SALMON. Digital data are available at JELA for SALMON but not for the Alabama earthquake. None of the paths are the same but both stations are located in the same general coastal crust and upper mantle region (Figure 23). Thus, for short distances the best alternative is to directly compare JELA (SALMON) with EUAL (Alabama earthquake), at distances of 2.19° and 2.82°, respectively.

In Figures 24 and 25 we show arrival times of various phases generated from dispersive filtering of signals at JELA

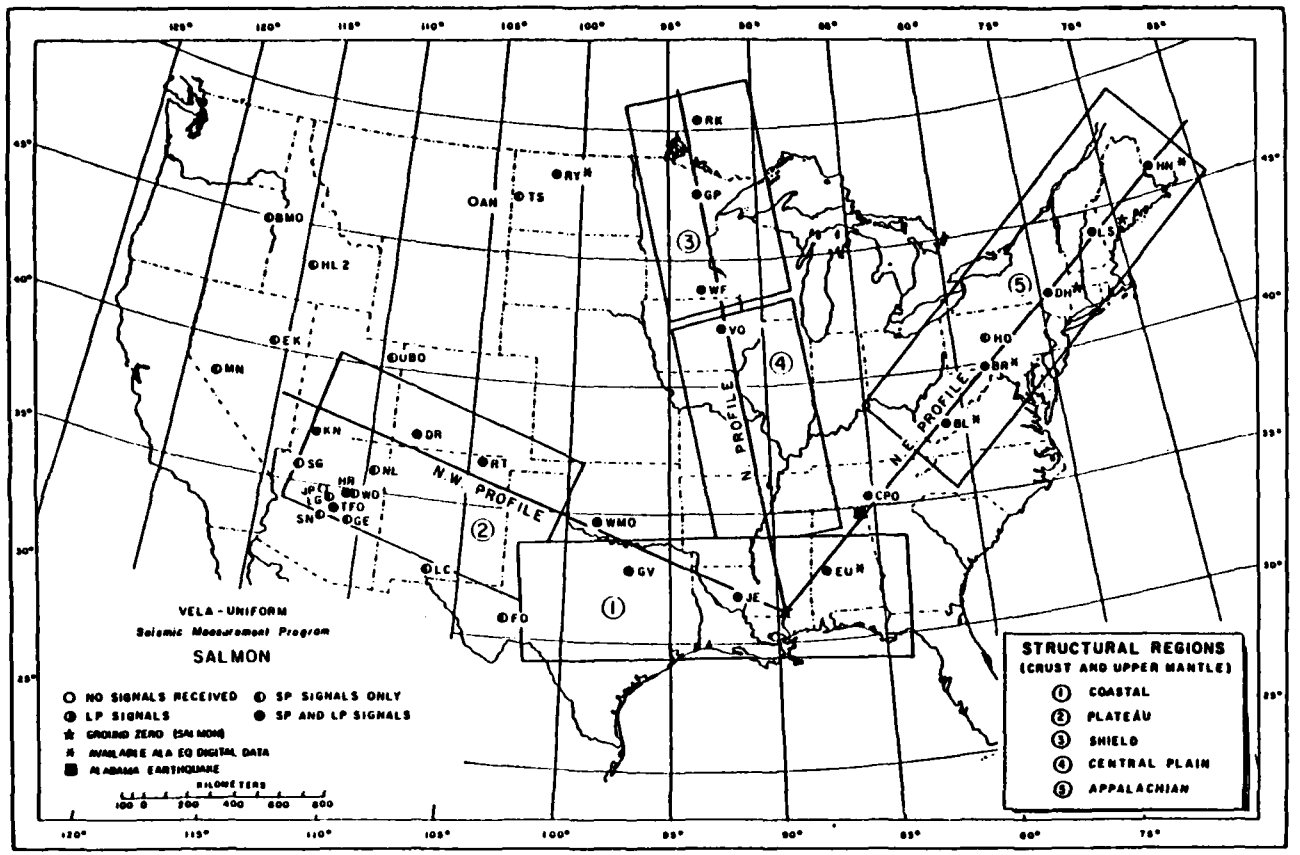

Figure 23. Station location, signal reception, structural regions, and station-source profiles.

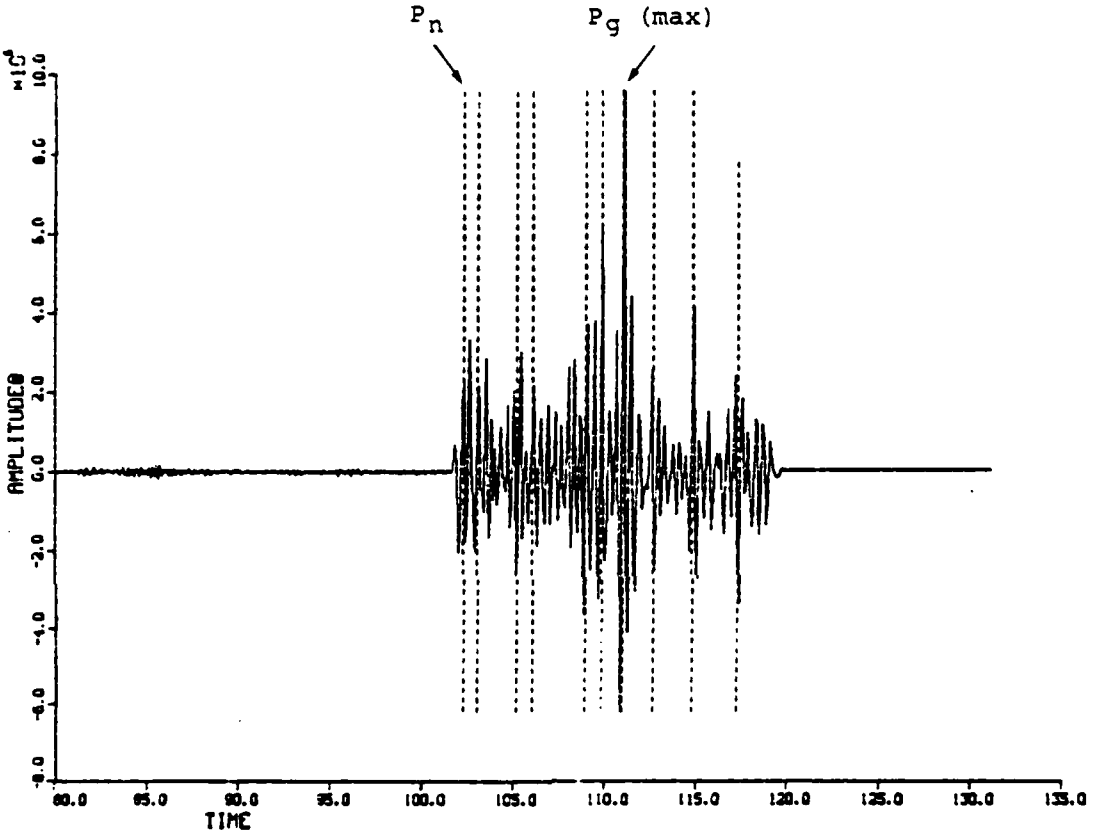

Figure 24. JELA, SALMON seismogram showing various phase arrival times generated by dispersion filtering using only "one pass" detection (Δ = 243 km, STA-EPI azimuth = 106°).

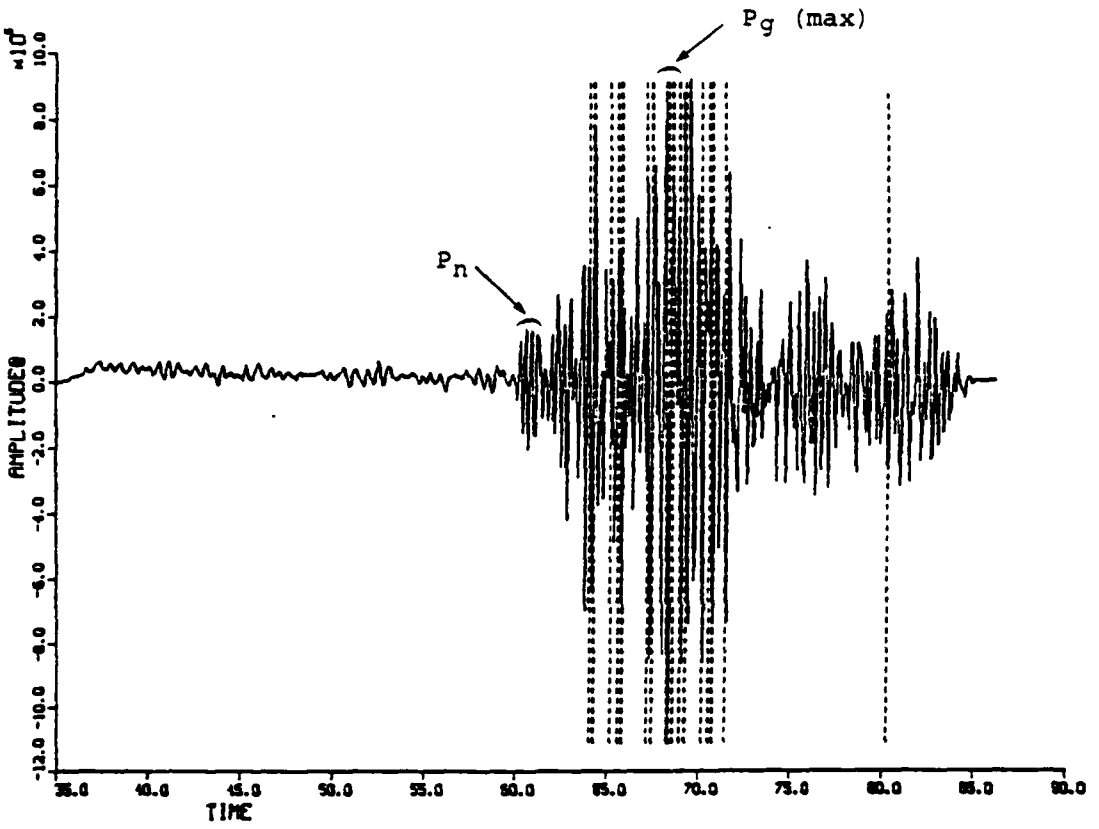

Figure 25. EUAL, Alabama earthquake seismogram showing various phase arrival times generated by dispersion filtering using "one pass" detection only (Δ = 314 km, STA-EPI azimuth = 44°).

and EUAL. The signals appear quite different in shape and size but not in frequency content. This is evident from narrow-band filter amplitude estimates shown in Figures 26 and 27. Figure 26 compares the maximum P_n pulse amplitude spectra for the two events and Figure 27 shows the maximum P_g pulse spectra.

To scale the spectra at a common distance, the JELA/SALMON P_n spectrum is divided by a factor of two based on an attenuation rate of $A \sim r^{-3}$ for the western United States (WUS) (Blandford, et al., 1980). The attenuation of P_n in the eastern United States is probably somewhat less, perhaps $A \sim r^{-2.5}$ (Blandford, et al., 1980) but a factor of two is adequate for the spectral comparison particularly since small differences in attenuation (t*) which may occur throughout the coastal region structure will not significantly change the character of the spectral differences. The P_g spectra for SALMON is divided by a factor of 1.5. This factor is based on the attenuation rate for P_g derived by Baker, 1970; also for the WES.

We observe that the SALMON P_n spectrum is greater in value and peaks at a higher frequency than the spectrum for the earthquake and this is true even if the spectra is averaged or smoothed. The P_g spectral estimates (for the P_g maximum pulse) from the two events are quite similar. This similarity in the maximum P_g pulse may be due more to the bandpass character of the structure transfer function than to similarity in the two source spectra. The former observation, however, suggests that the variable frequency magnitude discriminant applied to P_n may be effective for regional events. On the other hand, a spectral discriminant based on the maximum P_g pulse may not be useful. Many more station-event pairs will be required to verify these preliminary observations however.

Figures 28 and 29 show the seismograms and various arrival times obtained from dispersion filtering applied to

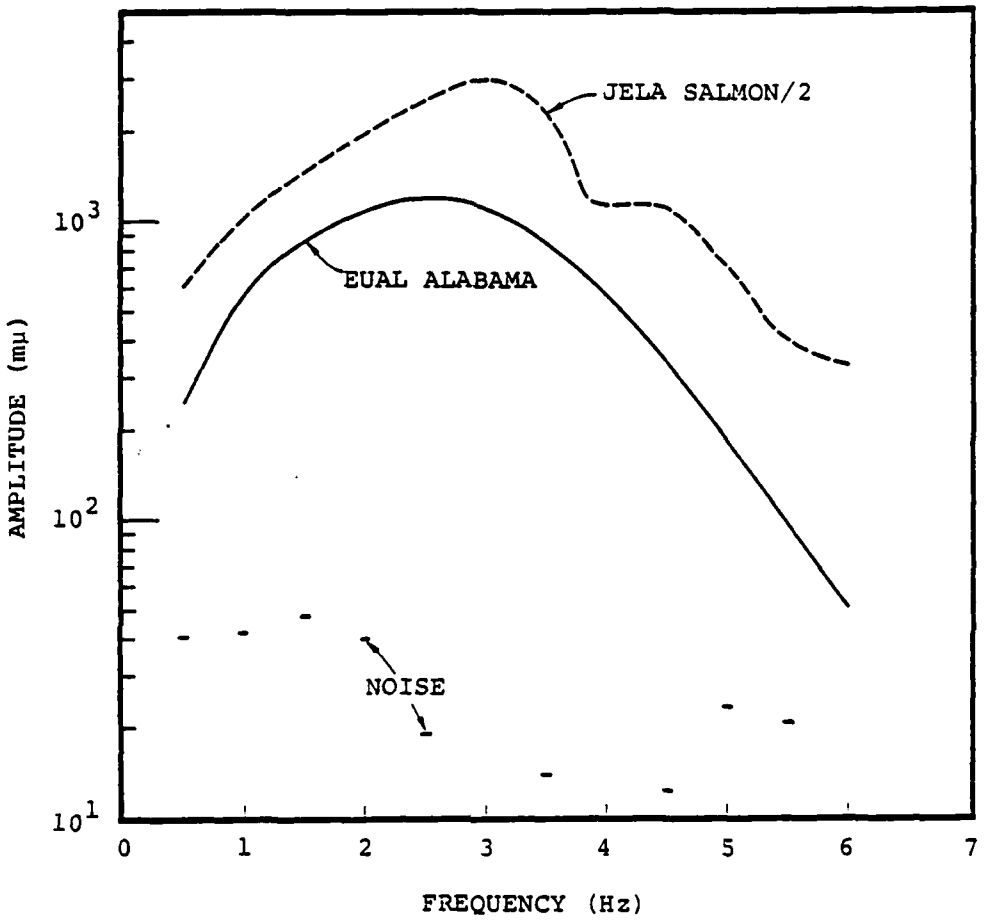

Figure 26. Narrow band filter generated P_n spectra at EUAL and JELA for the Alabama earthquake and the SALMON explosion.

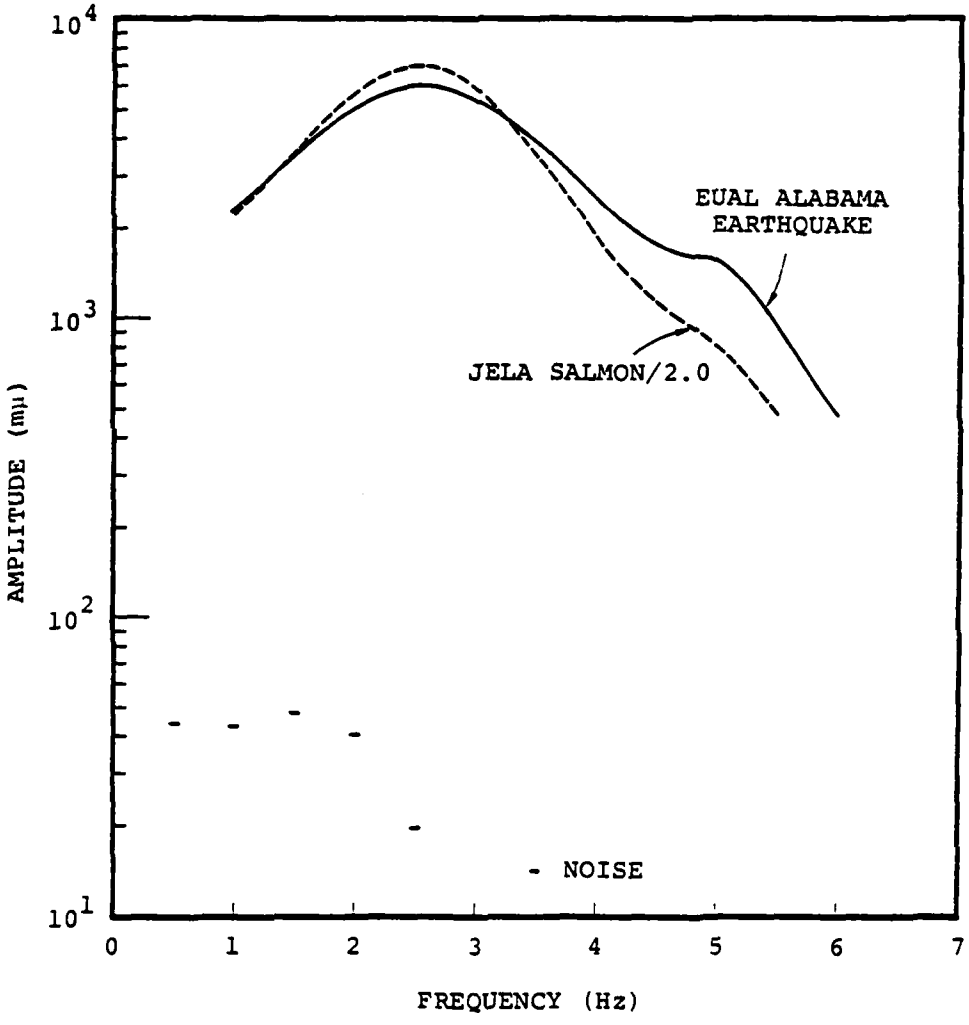

Figure 27. Narrow band filter generated spectra for the maximum P_g phase (U < 6.0 km/sec) at EUAL and JELA from the Alabama earthquake and the SALMON explosion.

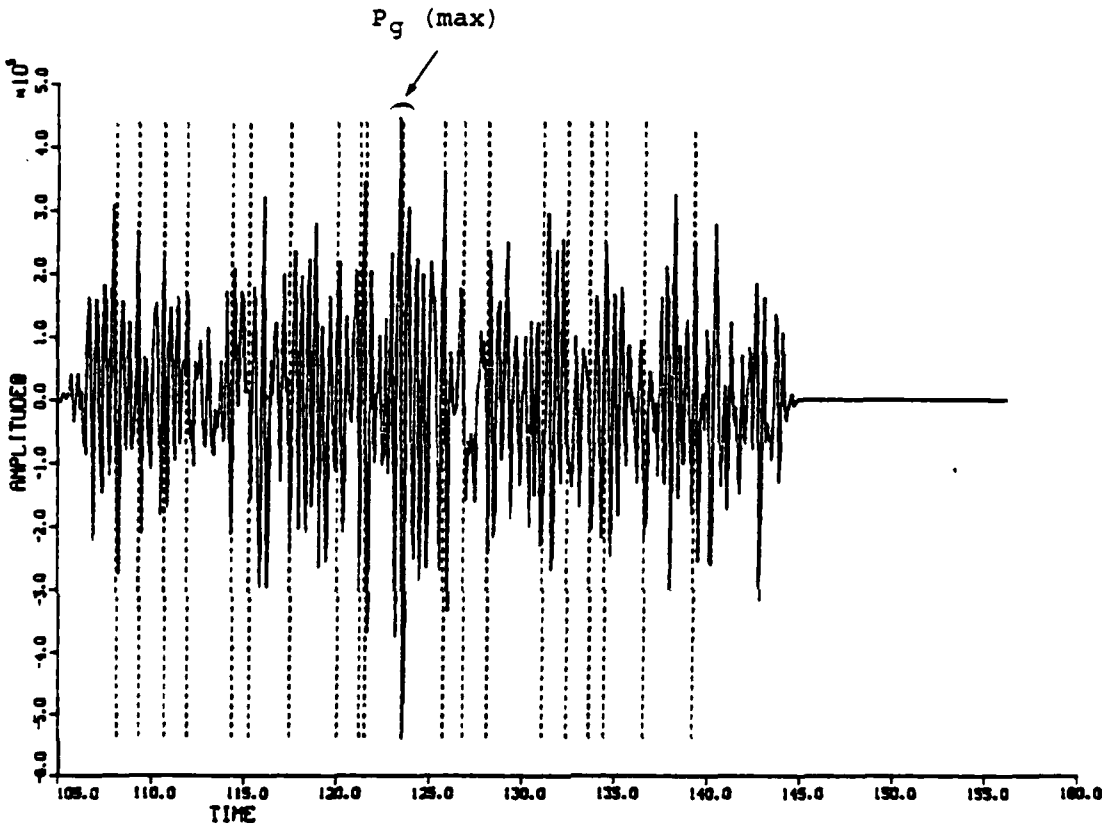

Figure 28. BLWV, SALMON seismogram showing various phase arrival times derived by first pass dispersion filtering (Δ = 1058 km, STA-EPI azimuth = 228°).

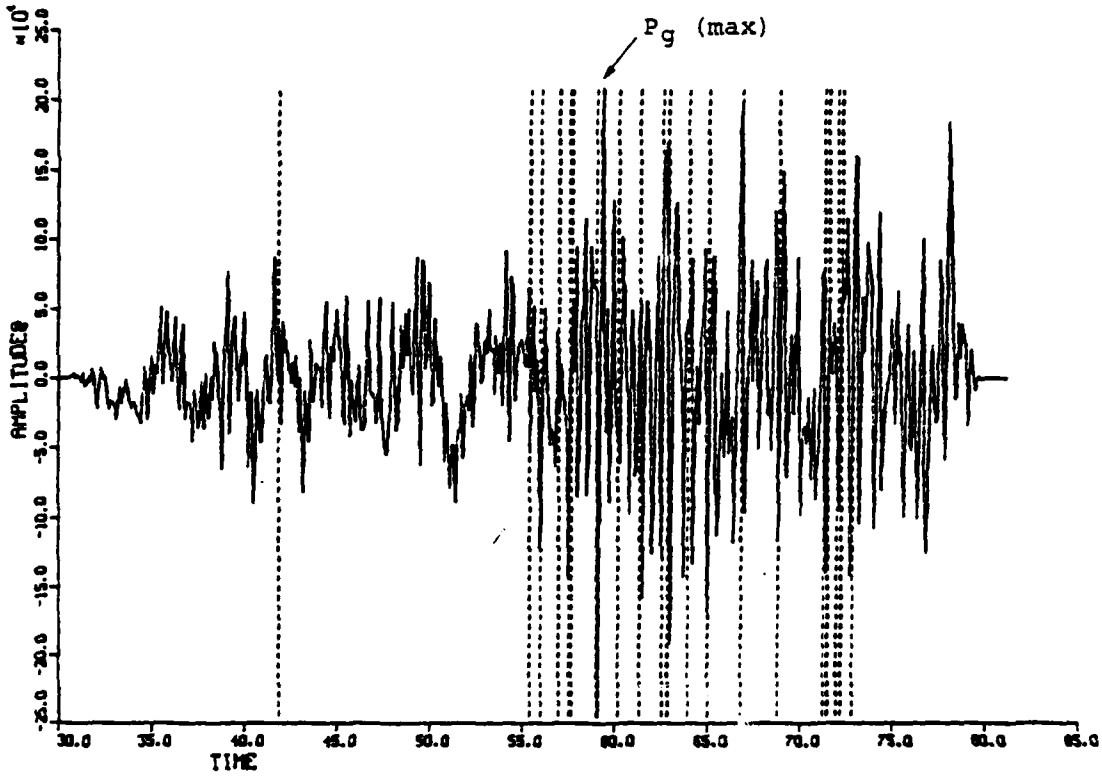

Figure 29. BR-PA, Alabama earthquake seismogram showing various phase arrival times derived by first pass dispersion filtering (Δ = 818 km, STA-EPI azimuth = 228°).

the two stations BLWV and BRPA, located at distances of 1058 and 818 kilometers from SALMON and the earthquake, respectively. The signals arrive at both stations from the same direction (i.e., STA-EPI azimuth = 228°). This event-station pair was selected for nearly equal distances and azimuths, again to minimize path effects. Granted the receiver and path transfer functions may differ (Figure 23) and a better selection would be SALMON/BLWV and earthquake/DHNY as far as distance and path are concerned, but again experimental realities interfer. That is the signal-to-noise (S/N) ratio is too low for the earthquake/DHNY record and as will be shown the S/N ratio is also low for BRPA.

The P_n phase at BRPA for the earthquake (Figure 29) is obscured by noise; however a larger signal is present for the P_g phase. In Figure 30, we compare the P_g peak amplitude spectra for the two events. The spectrum for BLWV/SALMON is divided by 1.5 to adjust for the existing distance difference (Baker, 1970). The BRPA P_g earthquake spectrum peaks at a slightly lower frequency than that at BLWV for the explosion, and generally shows larger amplitudes over the band of frequencies analyzed. However, in view of the rather low signal-to-noise ratio, it is probably not realistic to place much weight on these rather small differences. Rather, it seems most appropriate to investigate the possible P_g phase differences between the source types over more of the wavetrain (that is using more than just the maximum pulse within the wavetrain) and over a wider bandwidth, in particular at lower frequencies. These investigations are in progress, using more sophisticated quasi-harmonic decomposition methods.

In addition to the P_n and P_g phases, the L_g "phase" is a possible discriminatory arrival. Both P_g and L_g can be described as the superposition of a number of higher order P-SV or Rayleigh type modes (Press and Ewing, 1952 and Knopoff, et al., 1973). Alternatively, both can be described in terms

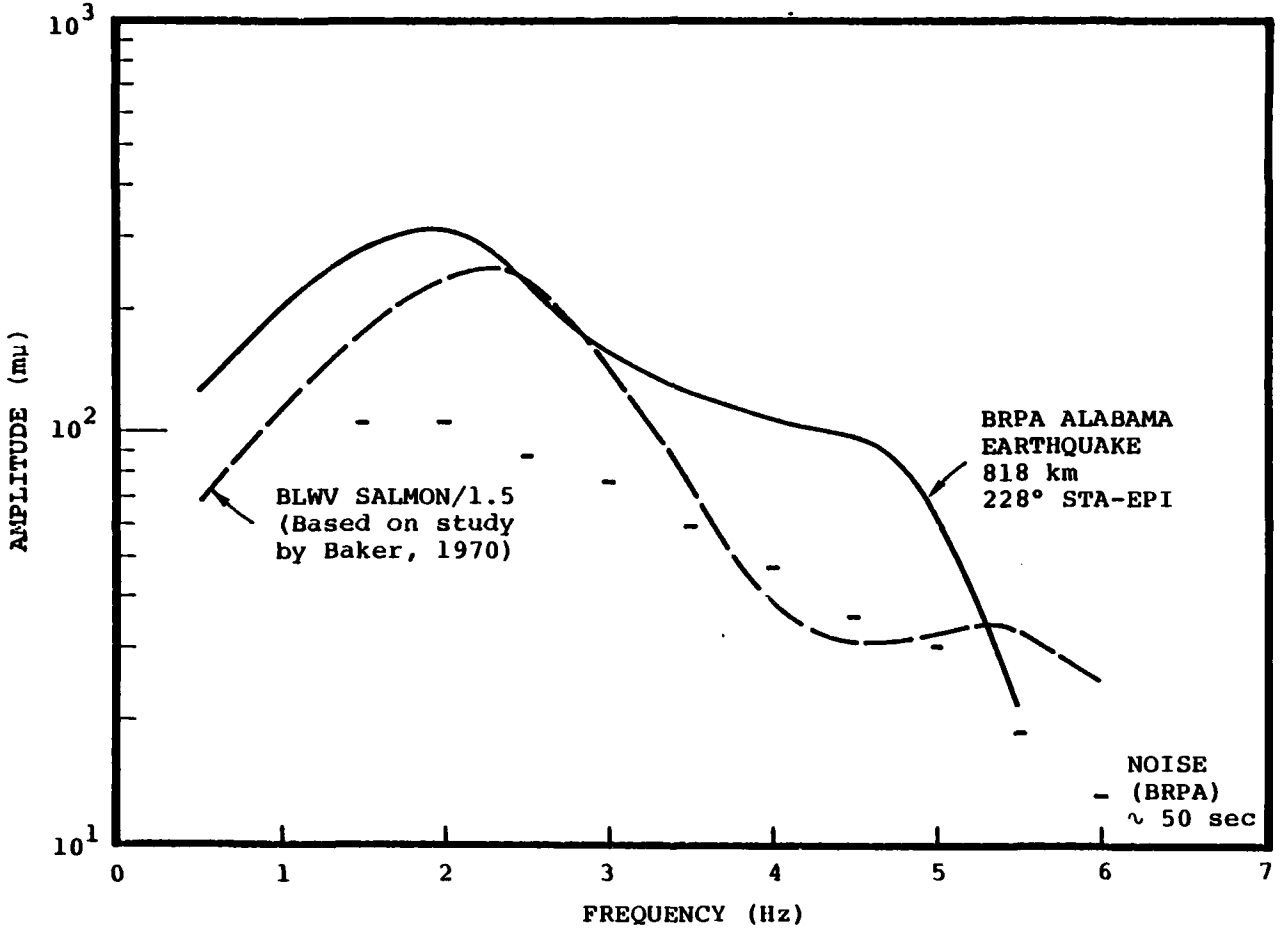

Figure 30. NBF spectra for the maximum P_g phase (U < 6.0 km/sec) at BRPA and BLWV for the Alabama earthquake and the SALMON explosion.

of a large number of multiple reflected body phases controlled primarily by P or S velocities, respectively (Archambeau, 1981; Helmberger and Enger, 1980).

Figure 31 shows the arrival times of pulses within an L_g group velocity window of 3.6 to 2.9 for the Alabama earthquake, recorded at BRPA. The spectrum of the maximum pulse in the L_g wavetrain is plotted in Figure 32, along with the maximum P_g pulse spectrum and the noise spectrum estimate for this event. The L_g spectrum peaks at a slightly lower frequency than P_g and is richer in low frequency energy. On the other hand, from preliminary time domain observations, the explosion event data appears to show L_g less than or comparable to P_g at most stations. This suggests that the relative excitation of the maximum P_g to L_g may serve as a useful discriminant. We currently are applying advanced signal isolation and spectral estimation methods (see Section 2.4.3 for example) to systematically verify these very preliminary observations.

The effects of receiver and source structure as well as crust-mantle characteristics on the ground motion at regional distances have been discussed by many authors. Additional, systematic characterization of these effects is indeed an important part of this study. However, because of the complex variations and indistinct character of many of the observed regional phases, measurements of other than simple peak amplitude spectral estimates will almost certainly be required for the development of robust regional discriminants. In this regard, energy estimates derived for isolated pulse arrivals and for the entire wavetrain are, and will be, investigated.

By way of example, simple integration of the wavetrain spectra over a frequency band for a specified time interval would tend to average out the effects of variations in propagation over different paths. For example, Figures 33 and 34 show L_g signals from two explosions, one in the EUS (SALMON) and the other in WUS (DIABLO HAWK) recorded at EUAL and

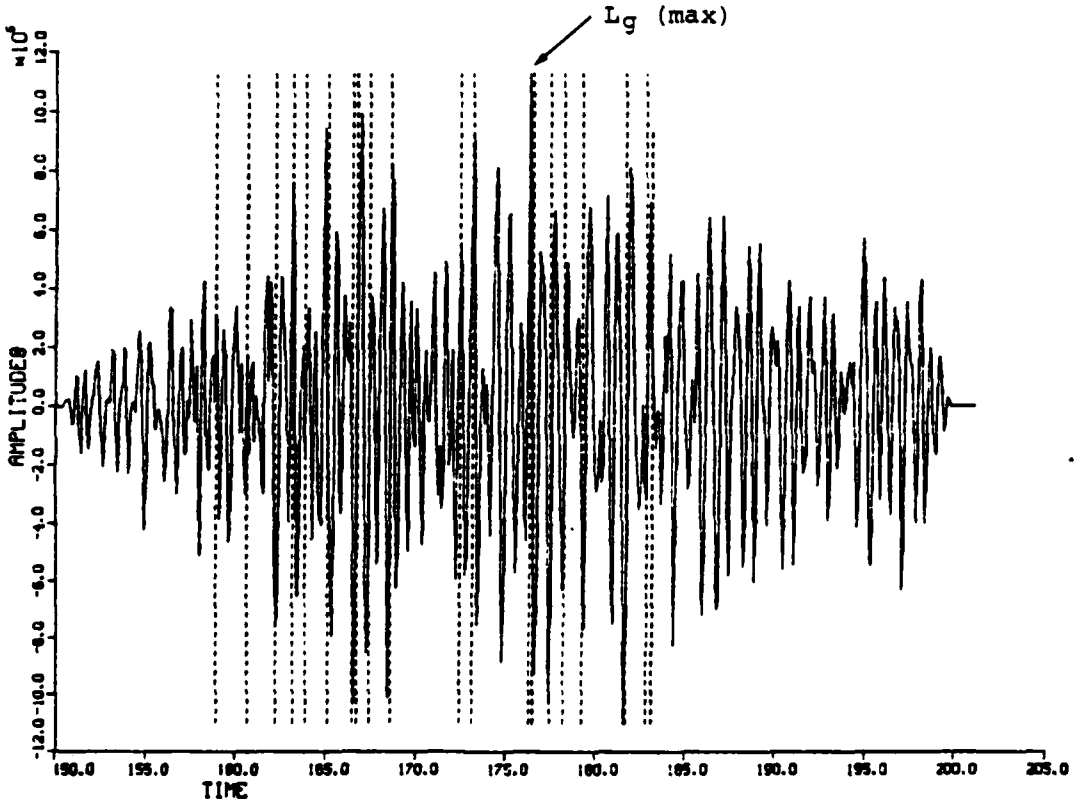

Figure 31. BRPA, Alabama earthquake seismogram showing various phase arrival times generated by dispersion filtering (Δ = 818 km, STA-EPI azimuth = 228°).

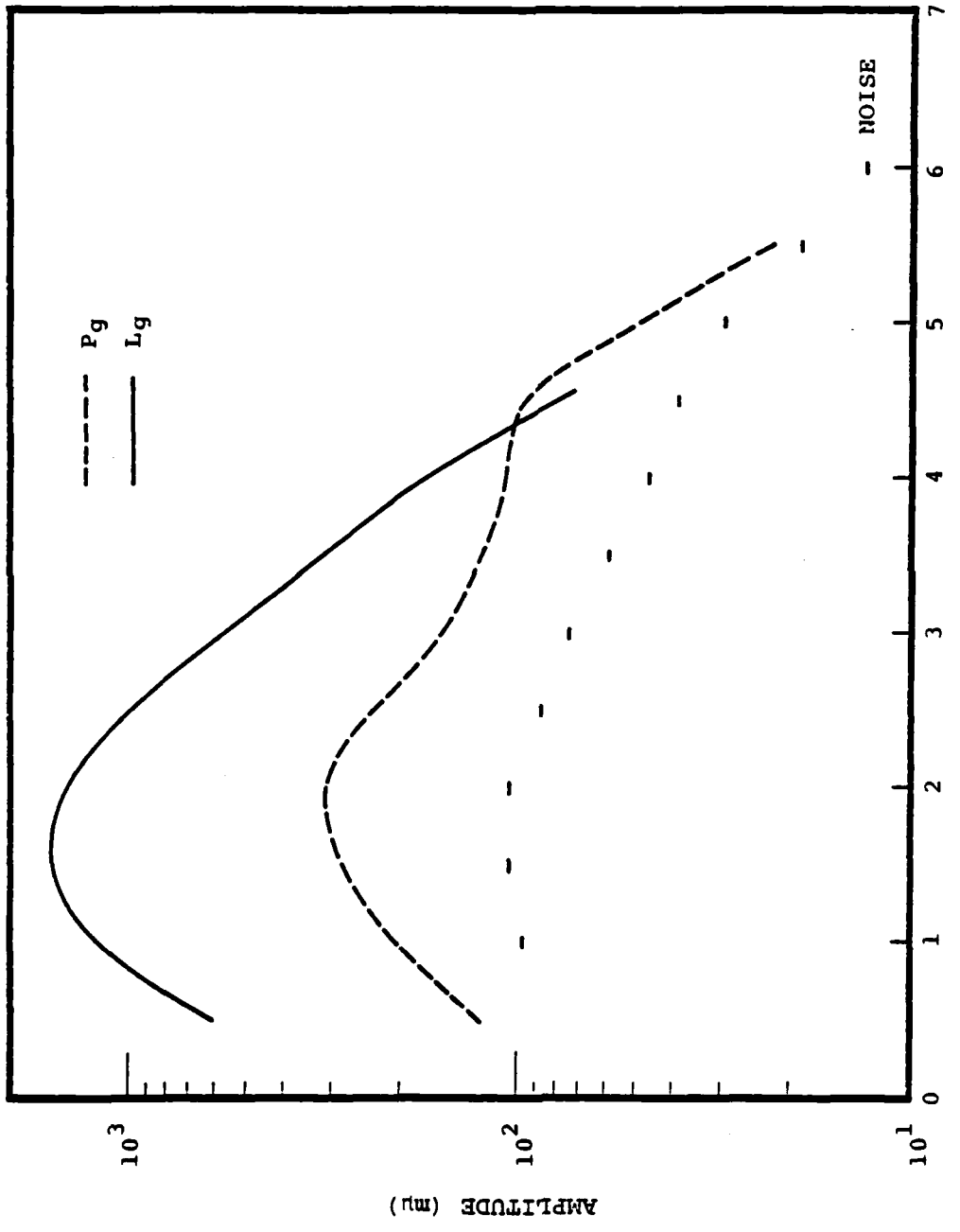

Figure 32. Maximum P_g, L_g (Rayleigh wave) pulse spectra at BRPA for the Alabama earthquake.

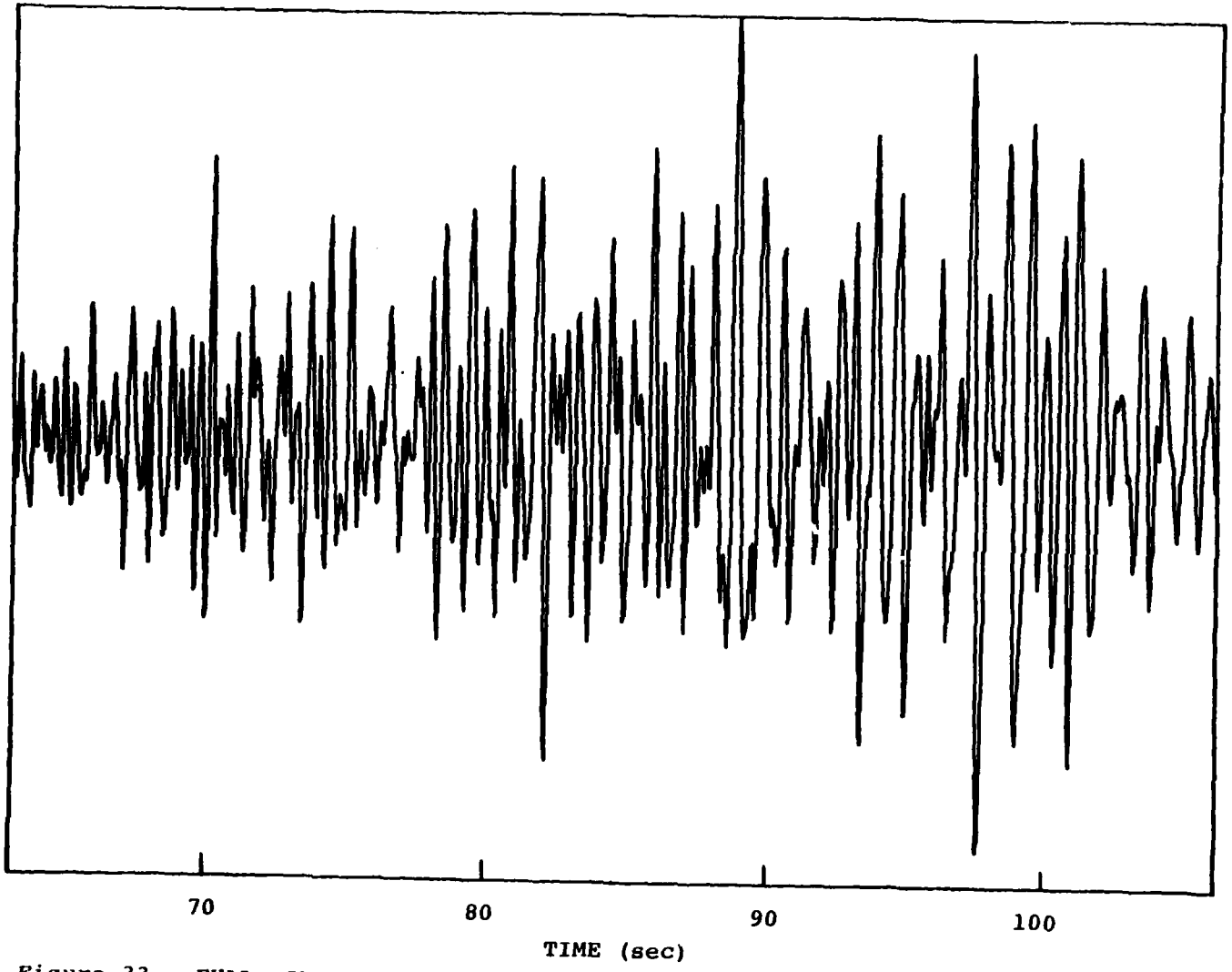

Figure 33. *EUAL, SALMON* seismogram for a group velocity window of 3.7 to 2.4 km/sec (Δ = 242 km, STA-EPI azimuth = 41°).

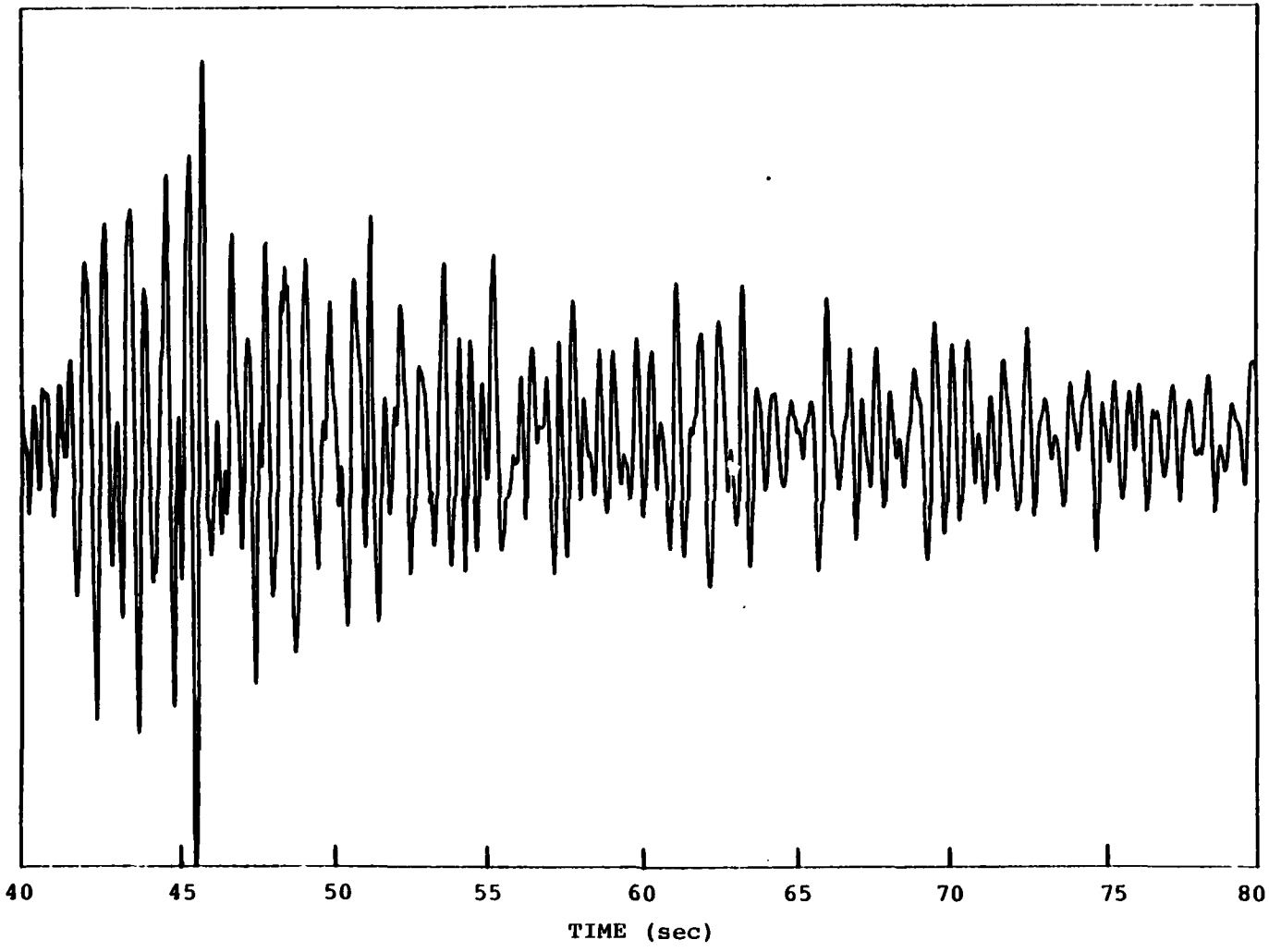

Figure 34. Minersville, DIABLO HAWK seismogram for a group velocity window of 3.5 to 2.4 km/sec (Δ = 303 km, STA-EPI azimuth = 250°).

Minersville, Utah, respectively. For the EUS (Figure 33), the L_g energy is relatively greater in the later portion of the wavetrain than for the early portion. The opposite is true for the WUS recording (Figure 34). The maximum-entropy moving-window spectra confirms these observations (Figures 35 and 36). The maximum-entropy moving window spectra is similar to a conventional sonogram analysis described by Cohen (1969). We expect, however, that proper summations over time would be independent of time shifts in the energy content due to propagation effects, and provide a stable estimate of the total recorded energy in the P_g and L_g wavetrains. In this case, we expect that the relative energy content of P_g to L_g will provide a good event discrimination variable. Our current and proposed work is directed to a systematic investigation of this and similar possibilities, as suggested by this preliminary work.

2.4.3 Regional Discrimination Using Advanced Quasi-Harmonic Decomposition (QHD) Methods

A more sophisticated form of the signal detection/analysis procedure has been developed (Archambeau, et al., 1981a) and is now incorporated in the MARS (Multiple Arrival Recognition System) program. We generally refer to the procedures involved in this time series analysis approach as multiple-pass dispersion filtering. The entire approach is based on quasi-harmonic decomposition of the time series, using narrow band filtering techniques, and is described quantitatively by Archambeau, et al., 1981b. The approach has great flexibility in that, when three component seismic data is available, both polarization and wave number filtering can be carried out jointly with the dispersion filtering to achieve a high degree of selectivity for signal detection and a large amount of signal information for all the signals detected. For regional data, where a large number of seismic phases arrive close to each other in time, it is not only desirable, but quite necessary, to isolate individual phases

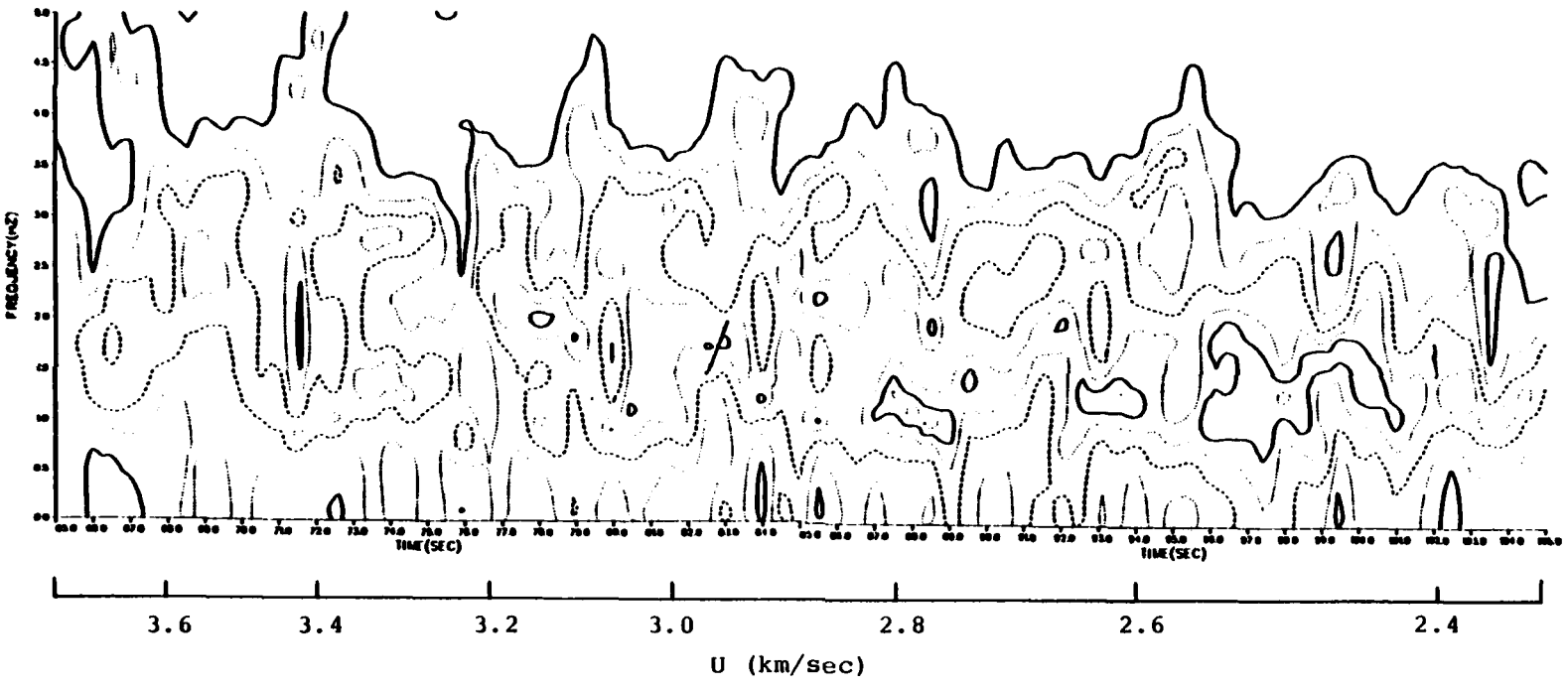

Figure 35. Contoured maximum entropy moving window spectral estimates of the L_g phase recorded at EUAL from the SALMON explosion (contour interval = 5 dB, Δ = 242 km, STA-EPI azimuth = 222°).

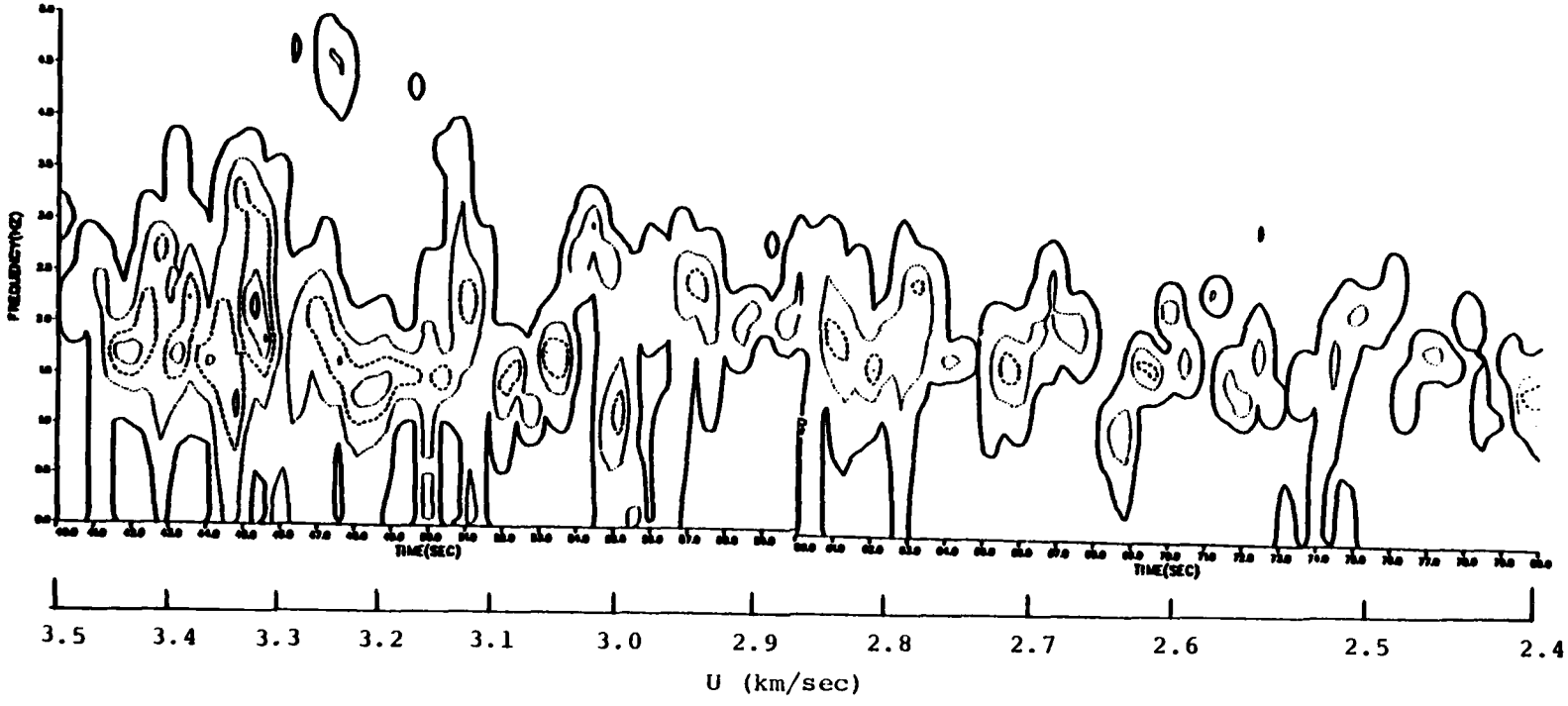

Figure 36. Contoured maximum-entropy moving window spectral estimates of the L_g phase recorded at Minersville, Utah from the DIABLO HAWK, NTS explosion (contour interval = 5 dB, Δ = 303 km, STA-EPI azimuth = 250°).

and obtain good (uncontaminated) estimates of the spectral content of each, their individual arrival times and sense of first motion, and, ideally, also their polarization, dispersion and wave number vector orientations as functions of frequency.

The new computer program developed has the capability of performing the entire complement of signal detection/analysis procedures mentioned. In the present framework, we are employing it to: (1) generate the signal data needed to define discrimination variables and location parameters for regional events, and (2) to investigate the robust character of candidate discrimination variables, using both real and synthetic seismic data, as functions of noise levels, event type and magnitude and structural variations. Ultimately, we also expect to use this program to automatically generate a subset of required discrimination variables to be used in a multivariate discrimination procedure for both regional and teleseismic events (Farrell, et al., 1981).

Figures 37 through 39 provide an example of the testing of this program for signal isolation and spectral analysis using regional synthetic seismograms. The objective here is to verify that the filtering correctly isolates regional type signal pulses in the presence of noise and obtains proper spectral estimates for each known signal pulse in the wavetrain. Figure 37 shows predicted ground motion as a function of distance from the source, in the near-regional distance range. The source was chosen, for this test, to be an explosion at great depth (10 km), so that the synthetic seismograms would be relatively simple. The method used to generate the synthetics is the locked mode approximation devised by Harvey, 1981. The phases arriving coherently across this distance range can quite easily be identified, so that at a given distance, it is possible to identify particular reflected, refracted and direct phases. (Phase identifications can also

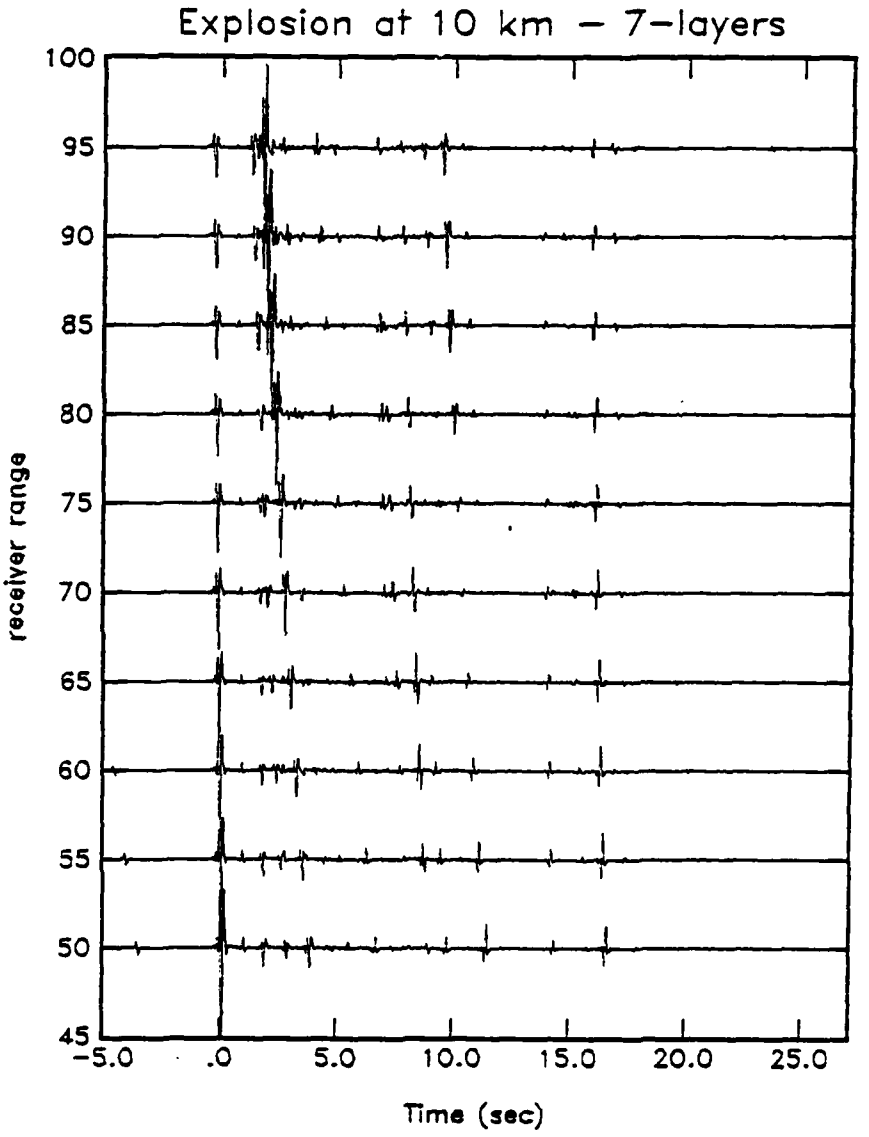

Figure 37. Synthetic near regional distance seismograms generated by mode superposition, for testing of signal detection and analysis methods.

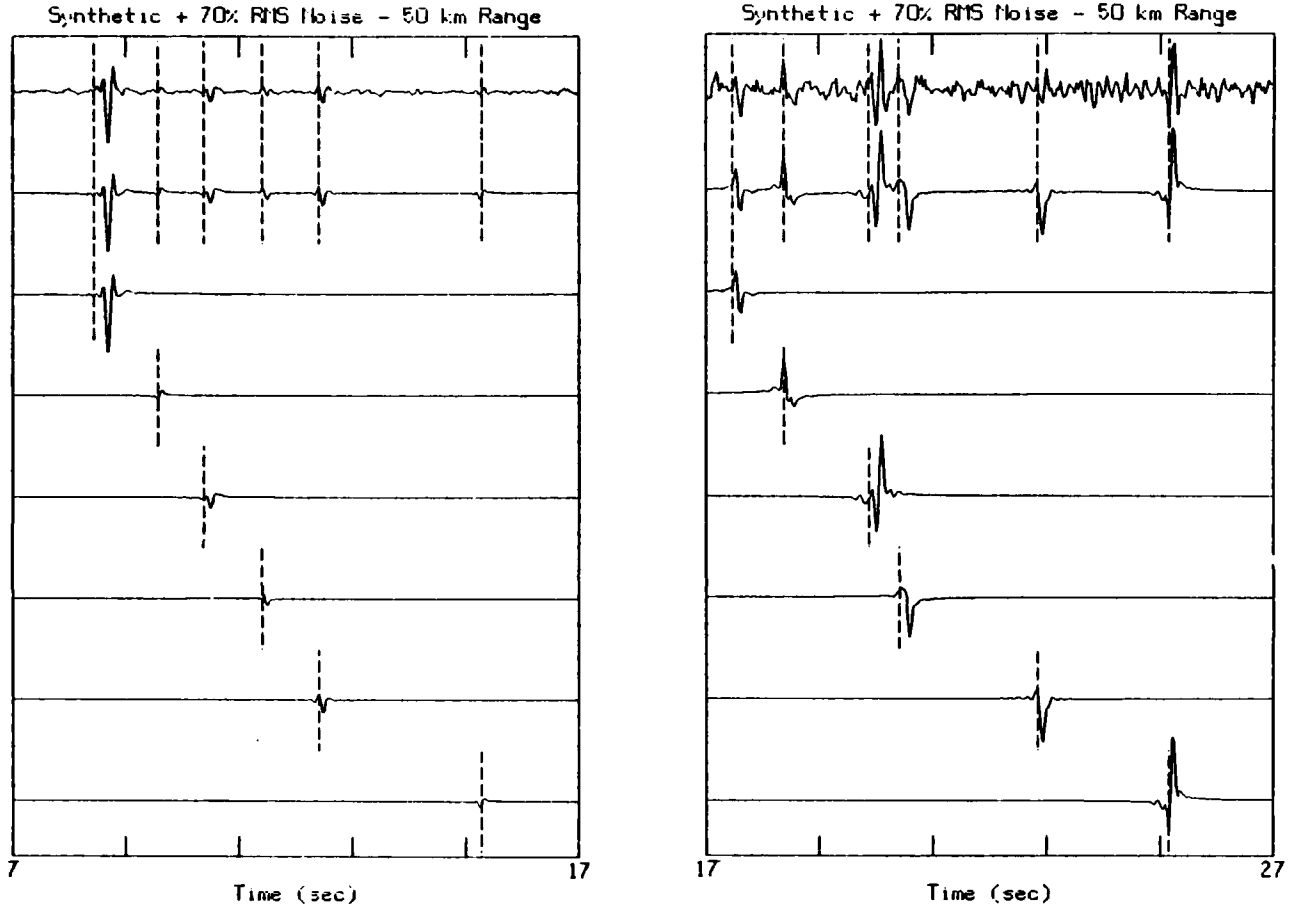

Figure 38. Synthetic regional seismogram with seismic noise added for testing of signal pulse isolation methods. The dotted lines denote automatically determined signal pulse arrival times. The top trace is the original data, the second trace is the superposition of the pulses obtained by dispersion filtering and the remaining six traces are the isolated pulse wave forms constructed from the pulse spectra estimated by QHD methods. The synthetic seismogram corresponds to that shown in Figure 36 at a distance of 50 km.

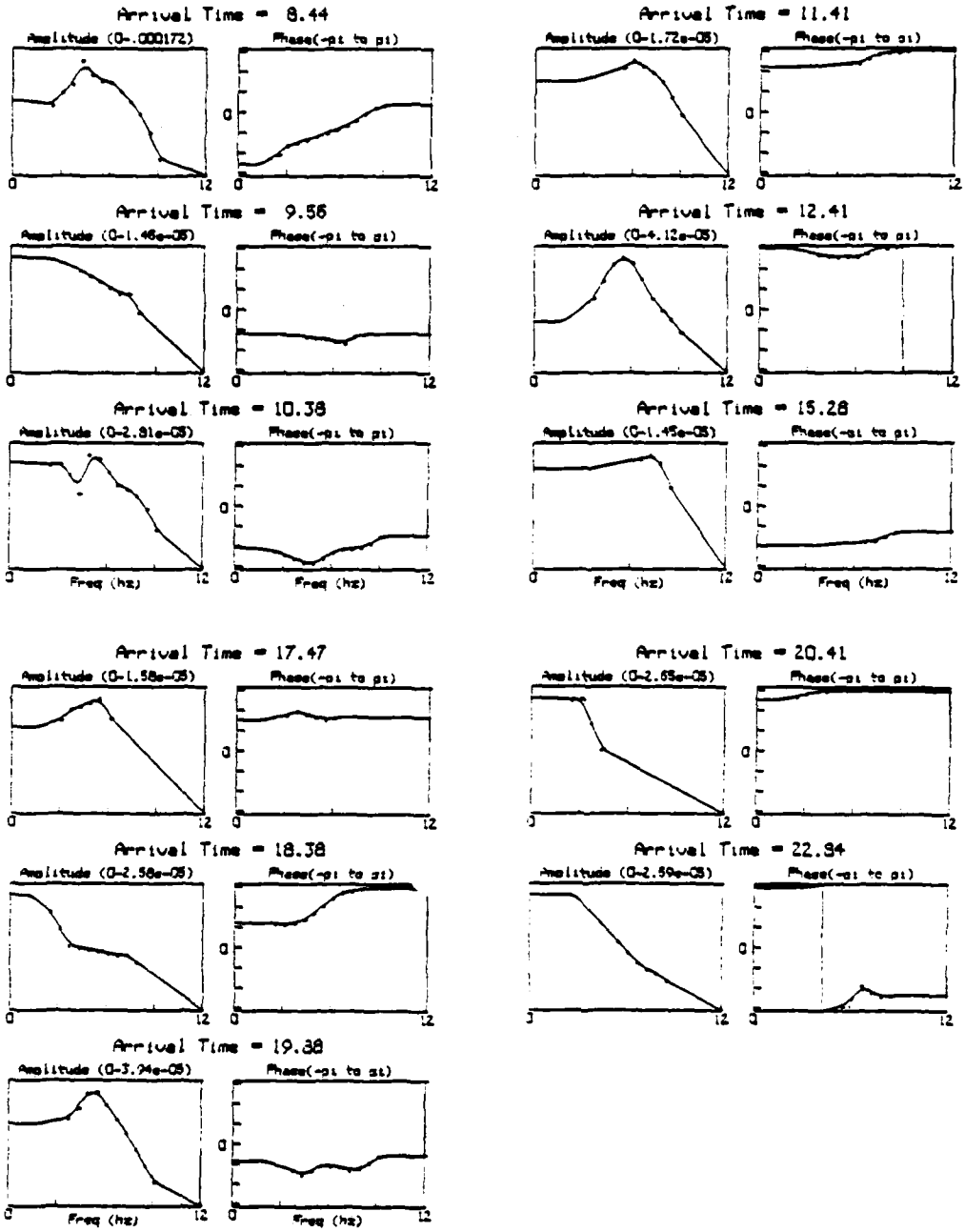

Figure 39. Signal pulse spectra as estimated by QHD filtering methods from the synthetic seismogram of Figure 37. The points are directly estimated from multiple narrow band filter output while the lines denote the interpolation-extrapolation of this data over the band 0 to 12 Hz.

be checked by theoretical ray tracing through the model velocity structure used.)

Figure 38 shows the results of adding seismic noise to the synthetic seismogram at 50 km from the source (top trace) and then processing the resulting time series through the dispersion filter procedure. In this operation, only pulse-like signals with little or no dispersion (i.e., body waves) are selected as signals of interest. The procedure involves ultra-narrow band filtering and generation of envelope and instantaneous phase functions from which the energy arrival times (group arrival times) and the spectral amplitude and phase at these times are measured and associated with the center frequencies of the narrow band filters. The desired undispersed pulses are then selected by a pattern search in the frequency-time-amplitude parameter space, with those pulses having the proper dispersion and preselected frequency dependent signal-to-noise threshold level being selected. Pulses are selected, their spectra subtracted from the origin data and the resulting "reduced" origin spectrum is inverted to the time domain. The entire filtering and search process is then repeated. This procedure is continued until no new signal pulses are found. (This iteration procedure is the origin of the term "multiple-pass dispersion filtering.") Pulses obtained in this way may overlap in time, and it is possible to separate phases that are time shifted by only a fraction of their apparent period. On the other hand, if the pulses are significantly smaller than the uncertainty or resolution time of the narrow band filter, then they are automatically combined together (spectrally added) at the end of the iteration process to form a single pulse. The individual pulse spectra so isolated are then inverted to the time domain, as shown in the lower six traces in Figure 38. In the figure these may then be summed to give a single time series, as in the second from the top trace in the figure, which can be

compared with the original. As can be seen from this comparison, the detection and isolation of the pulses by the filtering operations appears to be remarkedly accurate. This can also be verified by comparing the filtered output results with the original synthetic in Figure 37. Close examination shows that every significant pulse was detected and properly isolated with no false alarms. (One very weak arrival was, however, missed in the detection procedure, presumably due to its very low signal-to-noise ratio.)

Figure 39 shows the spectral estimates obtained for each of the pulses detected. That these spectral estimates are very reasonable estimates of the true spectra is apparent from the fact that when inverted to the time domain, they result in pulses that very closely match those of the pure synthetic, without noise.

In addition to the dispersion and spectral estimates of the isolated pulses, it is also possible to obtain the "times of arrival" of the phases. These are indicated by the dashed lines in Figure 38.

Figures 40 and 41 illustrate the application of the procedure to a small regionally recorded earthquake from Southern California. Only the first three seconds of the time series is shown in Figure 40 and within approximately a one second time interval five separate overlapping signal pulses are detected. The separate pulse waveforms are shown in the lower five traces, which have been inverted to the time domain from the spectral estimates shown in Figure 41. The sum of these pulses (second trace in Figure 40) is remarkedly similar to the first second of the event recording. The timing lines shown are computed in a manner designed to indicate where the maximum of the early arriving energy occurs, rather than at the signal pulse onset time.

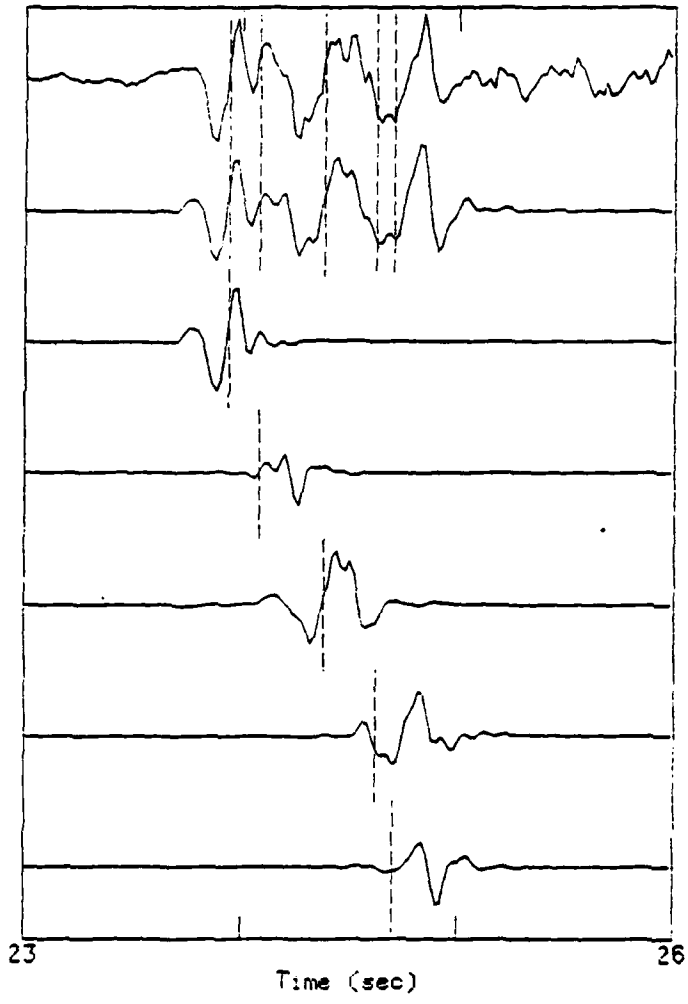

Figure 40. Regionally recorded seismogram ($\Delta \sim 100$ km) and signal pulses determined by multiple-pass *QHD* methods employing dispersion filtering. The top trace is the original earthquake data while the lower traces are time series constructed from the isolated pulse spectra. The second trace is the superposition of the single pulse results. The timing lines shown are determined automatically from (weighted) mean group arrival times for each pulse.

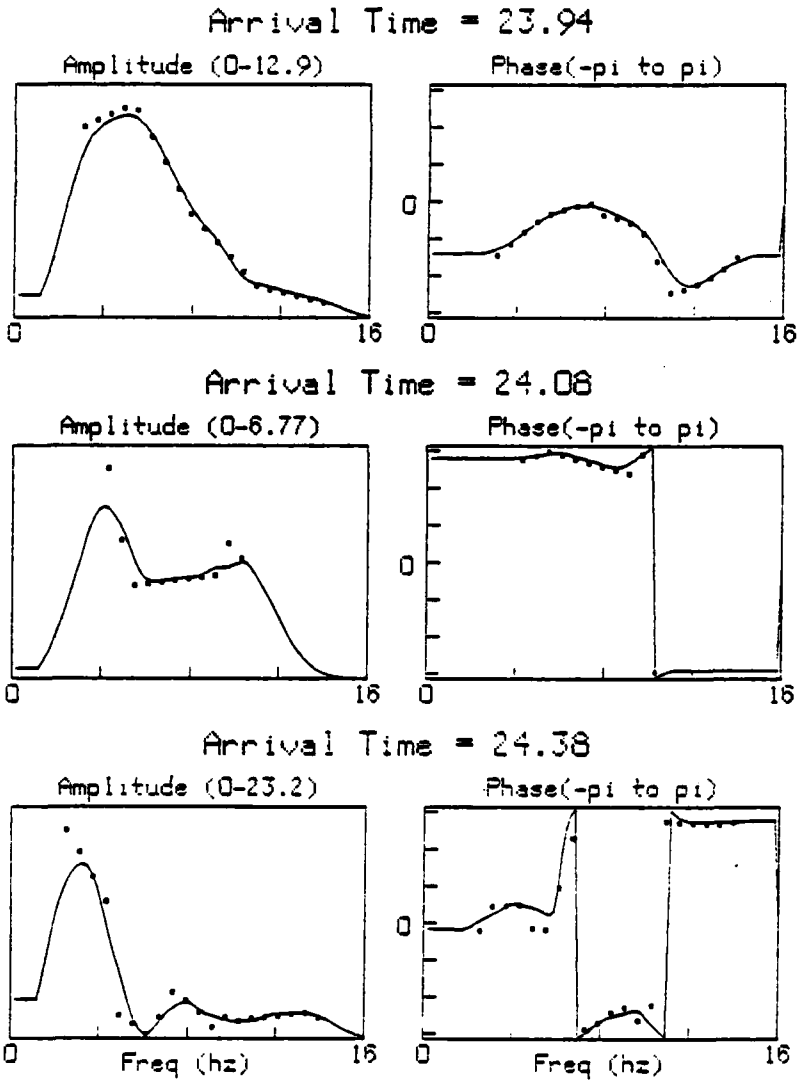

Figure 41. Signal spectra obtained by QHD analysis of the earthquake seismograms shown in Figure 40. The points are directly observed spectral estimates from the envelope function maxima and the instantaneous phase at the envelope maxima times. These spectral estimates are used to construct the first three isolated time domain pulses shown in Figure 40. The extrapolation criteria in the spectral domain requires zero spectral amplitude at zero frequency in order to obtain bandlimited results similar to those directly observed.

Figure 40 lists the arrival times of the isolated pulses and it is evident that they arrive within a few tenths of a second from each other.

It is evident from these examples that we are in a position to rapidly and accurately generate signal data, from which event discrimination and yield or magnitude results may be obtained. In particular, we clearly can measure frequency dependent magnitudes over a wide band of frequencies for any and all isolated phases. We can also automatically determine arrival times and first motion data for all of the phases quite reliably. We can, therefore, investigate spectral discriminants for P_n, P_g, S_n, L_g, R_g, etc. and, as well, obtain complexity measures, fault plane solutions and location and source depth estimates using all the phase information including S-P, pP, PP, etc. In this regard, we plan to form candidate discriminants and systematically test them against both real and synthetic regional seismic data.

III. SUMMARY OF CURRENT STATUS AND FUTURE STUDIES

3.1 REGIONAL PHASE CHARACTERIZATION

3.1.1 Introduction

As we described in previous sections of this report, development of a reliable discriminant using regional phase amplitude measurements has been hindered by the substantial scatter in the measurements and the lack of procedures for extrapolating experience from a tested area to a tectonically different untested area. In the future, we will investigate factors which might be responsible for the observed scatter, in the hope of developing corrections to the data which will permit a reduction in the scatter and hence result in a more reliable discriminant. Those factors which appear to contribute to the scatter include path attenuation, earthquake focal depth differences, earthquake focal mechanisms, source geologic environment and possible recording site conditions. It is our intention to analyze these factors using a well-controlled set of observational data and theoretical studies of the dependence of regional phase excitation and propagation on these factors.

3.1.2 Attenuation of Regional Phases

Our plan is to continue to develop a data base for describing the behavior of regional phase amplitude with distance for transmission paths crossing the U.S.S.R. We intend to categorize the available data according to tectonic regions. For this purpose, distinction will be made between paths crossing the platform and older fold areas and those crossing younger folded areas which, on the basis of our initial results, represent a clear difference in regional phase transmission properties. In particular, we will investigate in greater detail

the attenuation of regional phases leaving the Soviet Union to the south were stations important to the identification of small events in known Soviet nuclear testing areas may be located.

Using the available data we intend to develop a more quantitative description of the effects of attenuation on regional phase amplitudes. Such a description would ideally include identification of an effective Q such as described by Nuttli (1980) for various regional phases along paths from specific areas of particular interest (e.g., known Soviet test areas) to regional stations important to event discrimination in those areas. Where it is not possible to do this directly on the basis of published data, it may be possible to infer more quantitative Q estimates from regions of similar tectonics where the attenuation of regional phases is known. A firm basis for inferring attenuation properties could be established from additional theoretical analysis of regional phase transmission.

3.1.3 Variations in the Source

The principal factors to be considered here appear to be source depth differences and effects of focal mechanism on radiation pattern. As described in Section 2.3, the focal depth is expected to have significant effects on the excitation of certain regional phases. This is demonstrated for the L_g phase theoretically by the level of higher mode surface wave excitation from simple double couple sources at various depths of burial. We also noted a possible depth dependence in observations of the amplitude ratios of the L_g and P_g phases for events in Southern Californa. We are currently in the process of developing a data set covering a much larger range in focal depths using earthquakes in the Pamir-Hindu Kush area recorded at regional distances. It is our

intention to use measurements of regional phase amplitudes from these data to better characterize the dependence of excitation of various regional phases on source depth. For the L_g phase, we will compare the observations with theoretical computations of regional phase excitation based on the higher mode surface wave representation.

Finally, we will investigate the possible effect of variations in source radiation pattern in producing the observed scatter. Clearly, for earthquakes from a restricted source region we would expect this effect to be minor. However, in many of the studies using Soviet data, there is a large separation between earthquake sources which make up a common data set. Wherever data permit, we intend to take a closer look at possible mechanisms of individual events which contributed to these data sets. Using the higher mode excitation model, we will then assess the significance of mechanism differences in producing the observed scatter.

3.1.4 Application to Discrimination

Using the results of the above studies, we plan to analyze observations for a data base including earthquakes and explosions in the U.S.S.R. We will measure amplitudes of regional phases for the events in this data base. After making appropriate corrections for factors believed to contribute to the scatter, we will attempt to identify excitation differences between various regional phases for earthquakes versus the explosion sources. Finally, the reliability of any discriminant which is proposed from the data will be assessed in terms of the variability of the measurements and the significance of the correction factors which have been applied.

3.2 SPECTRAL DISCRIMINANTS BASED ON REGIONAL PHASES

One of our future objectives is to investigate spectral discriminants using more comprehensive regional data sets. In this regard, we will more thoroughly investigate VFM type discriminants, as well as other discriminants, for regional data, using large data sets (Caltech network data, LLL regional data and AEDS data as described in a separate section appended to this report) and synthetically produced "data," which can be systematically analyzed for definition of discriminants and their properties (e.g., "robustness") as functions of superposed noise levels, event type and magnitude, and source-receiver transmission characteristics. Among the "VFM" type discriminants to be used, which are essentially spectral discriminants involving differences in spectral excitation in two different narrow bands for the same phase, we are considering body wave magnitude ("$m_b(f)$") discrimination variables of the form:

$$x_k = m_b(f_k^H) - m_b(f_k^L) + b_k;\ k = 1, 2, 11, k \quad .$$

Here $m_b(f_k^H)$ and $m_b(f_k^L)$ denote magnitudes, for a particular body wave phase, at sets of high (f_k^H) and low (f_k^L) frequencies, and b_k are fixed constants. In general, a number of sets of high and low frequencies are used, so that the index k is used to label the various combinations of high and low frequency pairs. Definition of "discrimination variables" in this way is coupled to the use of multivariant discrimination methods, which are described by Farrell, et al. (1981).

Defined in this manner, we expect the mean $\mu_k(Q)$ (or median) of an earthquake "x_k population" to be less than the mean $\mu_k(E)$ of a similarly located explosion population. The constants b_k are used to adjust the variable for regional bias effects.

For regional events, we are considering this "$m_b(f)$ discriminant variable" for P, P_n, P_g, S and S_n type "body wave" phases.

In addition to the body wave VFM discrimination variables, we also will study similar surface wave type "VFM discriminants." In particular:

$$Y_\ell = M_s(f_\ell^H) - M_s(f_\ell^L) + B_\ell;\ \ell = 1,\ 2,..;\ L\ .$$

This very similar variable is defined in a completely analogous fashion as the "$m_b(f)$ discriminant." It is applied, for regional events, to both Rayleigh (R) and Love (L) type fundamental mode surface waves, including L_g (which is composed of higher order Rayleigh and Love modes).

In addition to the "VFM type" discrimination variables, we alsc consider the class of what can be termed the "m_b-M_s discriminants." These require mixed seismic phase measurements, involving magnitudes of two <u>different</u> seismic phases such as P_n and L_g or P_n and R at different frequencies. Thus, we consider discrimination variable sets of the form:

$$Z_n = \bar{m}_b(f_n^H) - \bar{M}_s(f_n^L) + C_n;\ n = 1,\ 2,..,\ N$$

where the magnitudes have essentially the same definitions as for the previously defined discriminants. In this case, however, the magnitudes maybe network averages.

For definition of Z_n for regional seismic data, we consider P_n, P, P_g and S, S_n for definition of an $\bar{m}_b(f_n^H)$, while R, L or L_g is used for $\bar{M}_b(f_n^L)$. As with the other discrimination variables, the expected population means or medians for explosions and earthquakes from similar regions is such that $\mu_n(E) > \mu_n(Q)$.

Finally, a number of other discriminants are being investigated, in particular, complexity type discriminants, depth discriminants involving time differences between early and later arriving phases in the seismogram, and time averaged energy differences between the more complex phases, such as P_g and L_g.

REFERENCES

Archambeau, C. B. (1981), Personal communication.

Archambeau, C. B., D. G. Harkrider and D. V. Helmberger (1974), "Studies of Multiple Seismic Events," California Institute of Technology Final Contract Report (Draft), prepared for the U. S. Arms Control and Disarmament Agency.

Archambeau, C. B., M. Schnapp, and R. Goff (1981a), "Computer Applications of Quasi-Harmonic Decomposition to Seismic Signal Detection and Analysis," to be submitted to Geophys. J. Roy. Astro Soc.,

Archambeau, C. B., J. M. Savino, J. F. Masso, and K. Hamilton (1981b), "Methods of Seismic Detection and Analysis Based on Quasi-Harmonic Decomposition (QHD)," submitted to Geophsy. J. Roy. Astro. Soc.,

Bache, T. C., H. J. Swanger and B. Shkoller (1980), "Synthesis of L_g in Eastern United States Crustal Models with Frequency Independent Q," Systems, Science and Software Semi-Annual Report submitted to the Advanced Research Projects Agency, SSS-R-81-4668, September.

Baker, R. G. (1970), "Determining Magnitude from L_g," BSSA, 60, pp. 1907-1919.

Barker, B., Z. Der and C. Mrazek (1980), The Effect of Crustal Structure on the Regional Phases P_g and L_g at NTS," in Studies of Seismic Waves Characteristics at Regional Distances, Teledyne Geotech Final Report, AL-80-1, Air Force Office of Scientific Research Contract F49620-79-C-0031.

Båth, M. (1954), "The Elastic Waves L_g and R_g along Euroasiatic Paths," Arkiv fur Geofysik, 2, pp. 295-342.

Båth, M. (1957), "A Continental Channel Wave, Guided by the Intermediate Layer in the Crust," PAGEOPH, 38, pp. 19-26.

Båth, M. (1959), "Seismic Channel Waves: New Obse-vations and Discussion," Gerlands Beit. zur Geophysik, 68, pp. 360-376.

Bennett, T. and J. Murphy (1980), " A Study of the Relative Excitation of Regional Phases for Use in Event Discrimination," presented at VSC Research Conference, November, 1980.

REFERENCES (continued)

Blandford, R., R. Hartenberg and R. Naylor (1980), "Regional Amplitude-Distance Relations, Discrimination and Detection," Teledyne Geotech Report SDAC-TR-80-6.

Blandford, R. and P. Klouda (1980), "Magnitude-Yield Results at Tonto Forest Observatory," in Studies of Seismic Wave Characteristics at Regional Distances, Teledyne Geotech Final Report, A1-80-1, Air Force Office of Scientific Research Contract F49620-79-C-0031.

Blandford, R. and R. Hartenberger (1978), "Regional Discrimination Between Earthquakes and Explosions (Abstract)," EOS, Trans. Am. Geophys. Union, 59, pp. 1140.

Blandford, R., R. Hartenberger and R. Naylor (1980), "Regional Amplitude-Distance Relations, Discrimination and Detection," Teledyne Geotech Report, SDAC-TR-80-6, (in press).

Cohen, T. J. (1969), "Seismoprint," SDL Report No. 238, Teledyne Geotech.

Farrell, W. E., J. Wang, C. B. Archambeau and R. C. Goff (1980), "Evaluation of the MARS Seismic Detector," Systems, Science and Software Technical Report SSS-R-81-4656, August.

Gupta, I. N., B. W. Barker, J. A. Burnetti and Z. A. Der (1980), "A Study of Regional Phases from Earthquakes and Explosions in Western Russia," BSSA, 70, pp. 851-872.

Harvey, D. J. (1981), "Seismograms Synthesis Using Normal Mode Superposition: The Locked Mode Approximation," Geophys. J. Roy, Astro. Soc. (in press).

Helmberger, D. and G. Engen (1980), "Modeling the Long-Period Body Waves from Shallow Earthquakes at Regional Ranges," BSSA, 70, pp. 1699-1714.

Knoppoff, L., F. Schwab and E. Kausel (1973), "Interpretation of L_g," Geophys. J. Roy. Astro. Soc., 33, pp. 389-404.

Nersesov, I. L. and T. G. Rautian (1964), "Kinematics and Dynamics of Seismic Waves to Distances of 3500 km from the Epicenter," Trudy Akad. Nauk USSR, Physics of the Earth, pp. 63-87.

Nuttli, O. (1980), "On the Excitation and Attenuation of 1-Hz L_g Waves from Sources in the U.S.S.R.," in St. Louis University Semiannual Technical Report No. 4, Air Force Office of Scientific Research Contract F49620-79-C-0025.

Nuttli, O. (1981), "On the Attenuation of L_g Waves in Western and Central Asia and Their Use as a Discriminant Between Earthquakes and Explosions," BSSA, 71, pp. 249-261.

Payo, G. (1960), "Estudio solre las Ondas Superficiales L_g, R_g, y Li en las Registras del Observatorio de Toledo," Ann. de Geofisica, 13, pp. 297-325.

Pec, K. (1961), "Continental Waves in Central Europe," Geophysikalni Sbornik, 152, pp. 123-192.

Pec, K. (1962), "On the Structure of the Kurile-Kamchatka Region According to L_g Wave Observations," Stud. Geophys. et Geodaet., 6, pp. 281-284.

Piwinskii, A. J. (1979), "Deep Structure of the Earth's Crust and Upper Mantle in the U.S.S.R. According to Geophysical and Seismological Data, Part I," Lawrence Livermore Laboratory Report UCID 18099.

Piwinskii, A. J. and D. L. Springer (1978), "Propagation of L_g Waves Across Eastern Europe and Asia," Lawrence Livermore Laboratory Report, UCRL-52494.

Pomeroy, P. (1979), "Regional Seismic Wave Propagation," Rondout Associates Semi-Annual Technical Report No. 3, Air Force Office of Scientific Research Contract F49620-78-C-0043.

Pomeroy, P. and T. Chen (1980), "Regional Seismic Wave Propagation," Rondout Associates Final Technical Report, Air Force Office of Scientific Research Contract F49620-78-C-0043.

Press, F. and M. Ewing (1952), "Two Slow Surface Waves Across North America," BSSA, 42, pp. 273-280.

Pshenikov, K. (1961), "L_g Waves According to Observations in Irkutsk," Geol. and Geofiz., 5, pp. 87-90.

Rijikova, S. (1966), "Velocities of the Seismic Waves Li, L_g and R_g Across the Aegean Sea," Bull. Inst. Geophys. Bulgarian Acad. Sci., 9, pp. 119-125.

Ruzaikin, A., I. Neresesov, U. Khalturin and P. Molnar (1977), "Propagation of L_g and Lateral Variations in the Crustal Structure of Asia," JGR, 82, pp. 307-31o.

Savarensky, E. and N. Valdner (1960), "Observations of L_g and R_g Waves from the Black Sea Basin Earthquakes," Ann. di Geofisica, 13, pp. 129-134.

Savino, J. M., C. B. Archambeau and J. F. Masso (1980), "VFM Discrimination Results for Eurasian Events Using the Priority 1 and Priority 2 Stations (U)," Systems, Science and Software Technical Report SSS-CR-80-4570.(S)

Savino, J. M., J. F. Masso and C. B. Archambeau (1979), "Discrimination Results From the Priority 1 Stations (U)," Systems, Science and Software Technical Report to ARPA, SSS-CR-79-4026. (S)

Sikharulidze, D. (1963), "The Nature of L_g and R_g Waves and the Study of the Crustal Structure," Trudy Institute Geofiz. Acad. Sci. Georgia S.S.R., 22, pp. 57-70.

Sutton, A. F. and W. M. Brady (1980), "Computer Program Development Specification for the Discrimination/Final Evaluation Subsystem (DFES) CPCI No. DFES001," Ensco, Inc. Report No. DCS-SFS-80-15.

Utsu, T. (1958), "On the L_g Phase of Seismic Waves Observed in Japan," Quart. Jour. Seis. (Japan), 23, pp. 61-76.

Utsu, T. (1960), "Observations of the L_g Waves and Crustal Structure in the Vicinity of Japan," Geophys Mag. (Japan), 29, pp. 499-508.

Valdner, N. and E. Savarevsky (1961), "On the Nature of L_g Wave and Its Propagation in Northeast Asia," Izvestiya Akad. Nauk SSSR, Series, Geofiz., 1, pp. 3-24.

Volvovsky, I.S. (1973), Seismic Studies of the Earth's Crust in the U.S.S.R.